Journal of African Earth Sciences 182 (2021) 104301

Contents lists available at ScienceDirect

Journal of African Earth Sciences

journal homepage: www.elsevier.com/locate/jafrearsci

# Bedrock petrology controls on hydrogeochemistry and fluoride concentrations in Precambrian aquifers of central Benin, Western Africa

Yao Yélidji Joël Tossou [a,b,e,*], Soulémana Yessoufou [c], Philippe Orban [a], Jacqueline Vander Auwera [d], Moussa Boukari [b], Serge Brouyère [a]

[a] University of Liège, Hydrogeology and Environmental Geology, Department ArGEnCO, Urban & Environmental Engineering, Building B52/3 - Sart Tilman, 4000, Liège, Belgium
[b] Université d'Abomey-Calavi, Institut National de l'Eau, Laboratoire d'Hydrologie Appliquée, 01 BP 4521, Cotonou, Benin
[c] Université d'Abomey-Calavi, Faculté des Sciences Techniques, Département des Sciences de la Terre, Cotonou, Benin
[d] University of Liège, Department of Geology (B20), Sart Tilman, 4000, Liège, Belgium
[e] Now at Sahara and Sahel Observatory (OSS), Boulevard du Leader Yasser Arafat BP 31, Tunis Carthage, 1080, Tunisia

ARTICLE INFO

*Keywords:*
Fluorine
Hydrogeochemistry
Mineralogy
Crystalline basement aquifer
Benin

ABSTRACT

In central Benin, fluoride concentrations in groundwater generally exceed the national and WHO guideline values (1.5 mg/L) and are locally above 7 mg/L (max. 7.19 mg/L). In this area, aquifers are found in a Precambrian bedrock made of migmatitic gneiss and granites. Recent hydrogeochemical studies have shown that the occurrence of fluoride in groundwater in this area is of geogenic origin. The aims of this investigation are to determine the sources of fluorine in the bedrock and to assess the role of geology on the mineralization and high fluoride concentrations in groundwater.

Thirty-five rock samples were collected in different areas that display contrasting concentrations of fluoride in groundwater. We carried out analyses of petrology, mineralogy and geochemistry on the samples. The results show that fluorine concentrations vary between 100 and 2900 ppm. Several fluorine-bearing minerals such as (biotite, muscovite, amphibole), titanite, fluorite, fluor-apatite, fluor-allanite, epidote and chlorite were identified. Groundwaters with elevated concentrations of fluoride are found in geological aquifers units and watershed rocks that contain fluorine bearing minerals. Biotite occurring in the granitic formations has the highest fluorine concentrations and appears as the most important contributor to the total fluorine from the bedrock to the groundwater.

## 1. Introduction

In Benin, as in many other countries around the world, groundwater is the main source of drinking water supply and groundwater quality must conform to national and international standards. In central Benin, the geological formations are mainly of Precambrian age and consist primarily of granite and migmatitic gneiss (Boukari, 1982; Bigioggero et al., 1988). Important aquifers are located in the fractured parts of these magmatic and metamorphic rocks. In these aquifers, abnormally high concentrations of fluoride (max. 7.19 mg/L) exceeding the national and the World Health Organization (WHO) drinking water guidelines value (1.5 mg/L) have been recorded (Dovonon et al., 2011). High concentrations of fluoride in drinking water causes dental fluorosis and, in extreme cases sekeletal fluorosis (Fawell et al., 2006; WHO, 2017; WHO, 2018). Around Central Benin, many cases of dental fluorosis are recorded (Dovonon et al., 2011). Recent hydrogeochemical and investigations (Tossou, 2016; Tossou et al., 2017) have demonstrated that the presence of fluoride in groundwater is mainly due to water-rock interactions (geogenic origin) and that fluorine concentrations in the main fertilizers used in the area is rather low (under detection limit, 0.1 ppm). Furthermore, a geostatistical study in the area supports a strong correlation between the spatial differentiation of the petrographic and textural characteristics of the basement rocks and the spatial distribution of groundwater mineralization (Tossou et al., 2019).

Fluorine occurs in many types of rocks (sedimentary, metamorphic and agneous). Fluoride is included in a variety of silicates or non-

* Corresponding author. University of Liège, Hydrogeology and Environmental Geology, Department ArGEnCO, Urban & Environmental Engineering, Building B52/3 - Sart Tilman, 4000, Liège, Belgium.
*E-mail addresses:* tossou_joel@yahoo.fr (Y.Y.J. Tossou), serge.brouyere@uliege.be (S. Brouyère).

https://doi.org/10.1016/j.jafrearsci.2021.104301
Received 3 October 2020; Received in revised form 5 June 2021; Accepted 6 June 2021
Available online 14 June 2021

**Table 1**
Main minerals of igneous rocks that contain fluorine together with their chemical formulae.

| Minerals | Chemical Formulae |
|---|---|
| Fluorite | $CaF_2$ |
| Cryolithe | $Na_3AlF_6$ |
| Apatite | $Ca_5(PO_4)(OH,F,Cl)$ |
| Topaze | $Al[SiO_4](OH,F)_2$ |
| Biotite | $K(Mg,Fe)_3(AlSi_3O_{10})(OH,F)_2$ |
| Muscovite | $KAl_2(AlSi_3O_{10})(OH,F)_2$ |
| Amphiboles | $(Ca,Na,K)_2(Mg,Fe,Al)_5[Si_6(Al,Si)_2O_{22}](OH,F)_2$ |
| Titanite | $CaTi[SiO_4](O,OH,F)$ |

silicates minerals (Lahermo et al., 2000; Edmunds et al., 2005). The principal minerals of igneous rocks that contain fluorine are listed in Table 1, together with their chemical formulae (Handa, 1975; Josephus Thomas et al., 1977; Susheela et al., 1999; Edmunds and Smedley, 2005). Minerals such as chlorite and clays could also contain fluorine in their structures (Edmunds and Smedley, 2005).

The average concentration of fluorine in the earth's crust ranges from 500 to 1000 ppm, however, some rocks like the Rapakivi granites in Finland may show fluorine concentrations of up to 5000 ppm (Bell et al., 1988). As in Finland, several other regions worldwide have geological formations with high fluorine concentrations.

The chemistry of groundwaters and specifically their fluoride concentration largely depends on the composition of the host rocks in the aquifers and watershed (Hem, 1985; Edmunds and Smedley, 2005; Karro et al., 2013a, 2013b). Therefore, it is important to investigate the mineralogy and geochemistry of the aquifer bedrock materials in which groundwater flows.

The aim of this study is to test the hypothesis that the mineralogy of the crystalline bedrock exerts a first order control on the fluorine content in groundwater of the study area. First, the geochemistry of fluorine and other major elements is investigated in the different geological formations of Central Benin. The second goal is to identify the type of geology and the main minerals that mostly contribute to groundwater mineralization and particularly, the main sources of high fluoride concentrations.

## 2. Description of the study area

### 2.1. Location, relief, hydrography and climate

The study area is located in central Benin and corresponds to the so-called "Département des Collines" (Department of Collines) administrative region. This department (Fig. 1) is situated between latitudes 7°27′ and 8°46′N and longitudes 1°39′ and 2°44′E (WGS 84/UTM zone 31N coordinate and projection system). The study area covers approximately 14 000 km$^2$ and includes six administrative districts (so-called communes): Bantè, Dassa-Zoumé, Glazoué, Ouessè, Savalou and Savè. According to data from the latest population census, there were about 700 000 inhabitants in the department (INSAE, 2013).

The landscape is a relatively homogeneous peneplain on the Precambrian bedrock, with an average elevation (relative to sea level) varying from 170 m in the north to 60 m in the south. There are series of scattered inselbergs with abrupt slopes, mainly in Dassa-Zoumé, Savè, and Savalou, and small chains of hills that can extend over longer distances (more than 10 km). The highest elevations are located at the mountain summits in Dassa-Zoumé (465 m), Savalou (520 m) and Savè (400 m) (Dubroeucq, 1977; Igue et al., 2001; Oloukoi et al., 2006). The main rivers of the region (Zou and Ouémé rivers and their tributaries)

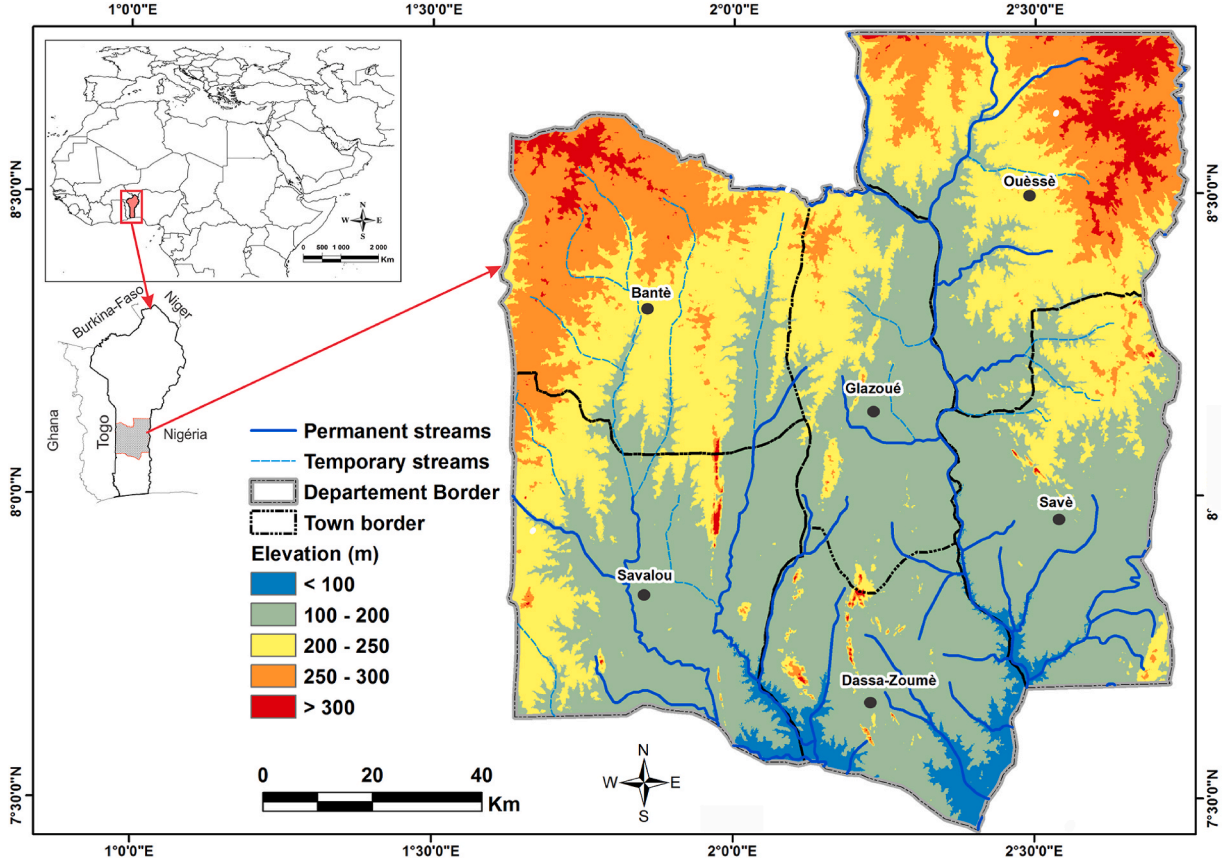


**Fig. 1.** Location of the Department of Collines in Benin and Sub-Saharian Africa together with the elevations and hydrographic networks of the studied area. The inserts show the location of Benin in Africa.

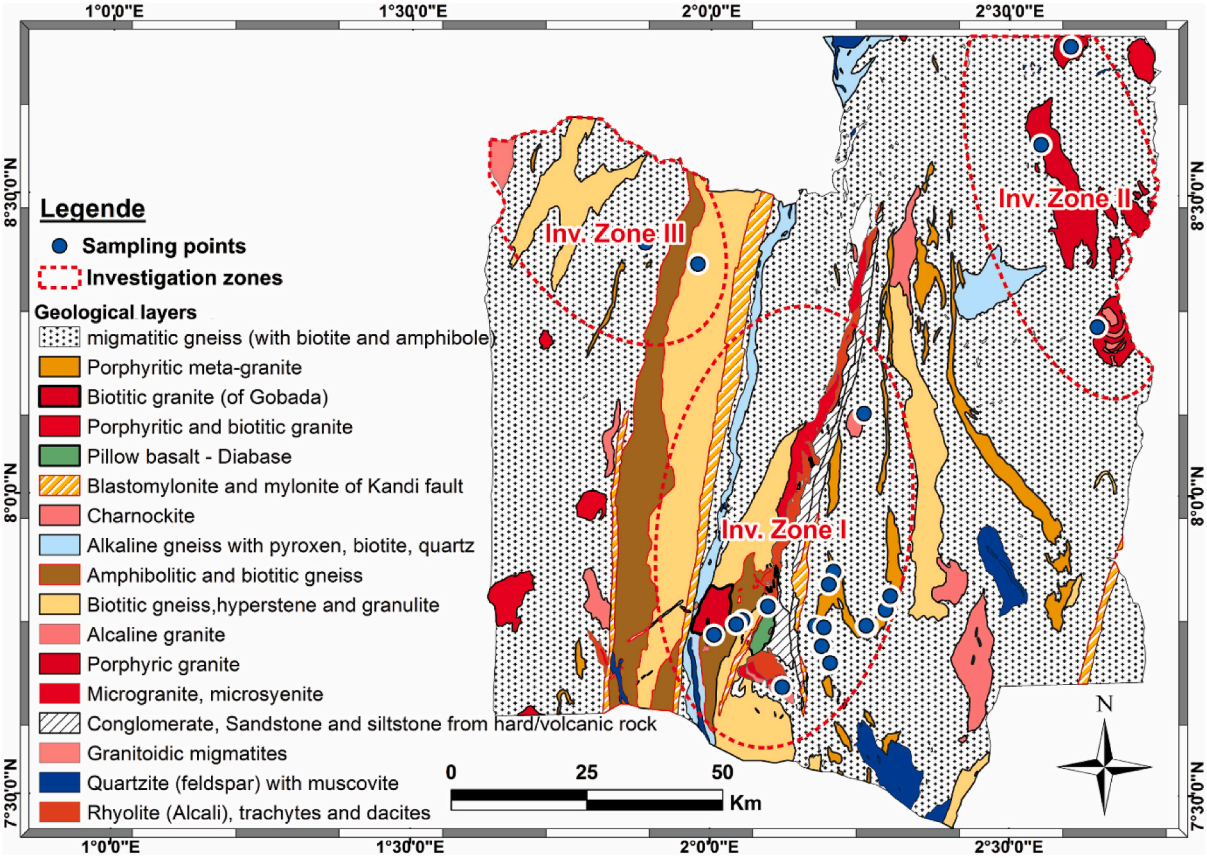


**Fig. 2.** Geology of the study area and sampling locations for rock samples. **Inv. Zone** in the map refers to the Investigations Zones (see section on Methodology). To make it short, "IZ" will be used instead of "Inv. Zone".

flow from a north to south direction. Most of tributaries and sub-tributaries dry up completely during the dry season (Barbé (Le) et al., 1993).

The climate of the region is mainly of Sudan-Guinean type characterized by one rainy season from May to October and one dry season from November to April. The mean annual rainfall over the last three decades (1981–2015) has been 1100 mm (data from *Agence Nationale de la Météorologie du Bénin*[1] at Savè climate station). Temperature varies from 22 to 36 °C, with an average value of 29 °C. The annual mean actual evapotranspiration (AET) is approximately 1000 mm over the period from 1981 to 2015.

### 2.2. Geology

The study area belongs to the "Structural unit of the Bénin plain" and consists of complex geological formations at both regional and local scales (Fig. 2). Several phases of deformation, metamorphism and magmatism have affected the different geological formations (Boukari, 1982). The area is dominated by three main geological units of Precambrian age (500–600 Ma) consisting of migmatites, gneiss and granites (Bigioggero et al., 1988; Faure et al., 1996).

The southern part of the area (below latitude 8°), is overlain, to a large extent, by migmatitic and gneissic formations with some circumscribed granitic plutons. This area also contains sedimentary formations restricted to a narrow tectonic basin, the so-called Idaho-Mahou basin (Breda, 1989) ***cited in*** Adissin Glodji et al. (2014).

The north-eastern region is characterized by scattered porphyritic and biotite granite plutons emplaced in migmatites and gneisses. In the north-western region, only migmatite and gneisses are present (anatexites of the group of Pira) (Fig. 2).

Gneisses and migmatites have a variable composition including: (i) biotite- and hypersthene-bearing gneisses in some places; (ii) biotite and garnet-bearing gneisses; (iii) alkaline gneisses with pyroxenes, amphibole and epidote, garnet gneisses, alkaline biotite gneisses with quartzites and marbles; (iv) massive amphibole-bearing gneisses and banded amphibole- and biotite-bearing gneisses containing amphibolite and pyroxenite enclaves and charnockites (Breda, 1989) ***cited in*** Adissin Glodji et al. (2014).

The granites have variable mineralogy and grain size (porphyritic or fine-grained and sometimes deformed locally). The important plutons are located closed to Dassa-Zoumé (Dassa, Tré, Fita and Gobada massifs) (Bigioggero et al., 1988; Adissin Glodji, 2012).

In the vicinity of Dassa-Zoumé, there is the so-called Idaho-Mahou volcano-sedimentary basin which is a limited to a narrow tectonic basin and consists of volcanic and weakly metamorphic sedimentary formations. It is north - south oriented with a length of about 100 km and a width up to 10 km (Adissin Glodji et al., 2014). According to Boussari (1975), the basin is filled with metavolcanic rocks (basalts and rhyolites) and metasediments (conglomerates, sandstones, silts) and intruded by microgranite and fine-grained gabbros. All these rocks underwent metamorphic green schist facies conditions in the late Neoproterozoic (Adissin, 2014). The mineralogy of granites is dominated by quartz, biotite, feldspars, amphibole and accessory ilmenite, titanite, epidote, apatite, and fluorite (Boussari, 1975; Bigioggero et al., 1988).

Boussari (1975) established that the gneisses are the oldest units, followed by the migmatites (produced from migmatisation of the gneisses) and lastly, the granites. The metasediments belonging to the bedrock consist of detrital, sandy or clayey sandy and lateritic soil. They are also associated with mafic and felsitic volcanic rocks.

[1] http://meteobenin.bj/.

**Table 2**
List of samples together with their locations, natures of rock and type of analyses applied to each of them.

| Samples | I.Z | Xcoord | Ycoord | Rock type | Thin sections XRD and Fluorescence | Electron microphobe | Electron scanning microscope (SEM) | point counting |
|---|---|---|---|---|---|---|---|---|
| BA1 | 3 | 2.1923 | 7.7762 | Migmatitic gneiss with biotite and amphibole | × | | | |
| BA2 | 3 | 2.2023 | 7.7821 | Biotitic gneiss with garnet | × | × | | |
| BA3 | 3 | 2.2152 | 7.8214 | Migmatitic gneiss with biotite and amphibole | × | | | |
| BA4a | 3 | 2.2633 | 7.782 | Migmatitic gneiss with biotite and amphibole | × | | | |
| BA4b | 3 | 2.2569 | 8.1364 | Migmatitic gneiss with biotite and amphibole | × | | × | |
| BA4c | 3 | 2.5526 | 8.5845 | Migmatitic gneiss with biotite and amphibole | × | | | |
| BA4d | 3 | 2.2066 | 7.8735 | Migmatitic gneiss with biotite and amphibole | × | | | |
| DZ10 | 1 | 2.0542 | 7.7919 | Porphyric granite | × | | × | |
| DZ11 | 1 | 1.9786 | 8.3849 | alkaline granite | × | | × | × |
| DZ12 | 1 | 2.1986 | 7.8518 | alkaline rhyolites | × | | × | |
| DZ13a | 1 | 2.187 | 7.7491 | Porphyric granite | × | | | × |
| DZ13b | 1 | 2.187 | 7.7491 | Porphyric granite | × | | | × |
| DZ14 | 1 | 2.1756 | 7.7831 | Wheathered sample | × | × | × | |
| DZ1a | 1 | 2.1907 | 7.7804 | Porphyric granite | × | | | × |
| DZ1b | 1 | 2.2011 | 7.7213 | Porphyric granite | × | × | | |
| DZ2 | 1 | 2.2624 | 7.7813 | Porphyric granite | × | × | | |
| DZ3 | 1 | 2.2612 | 7.7833 | Porphyric granite | × | | | × |
| DZ4a | 1 | 2.2936 | 7.8097 | Porphyric granite | × | | | |
| DZ4b | 1 | 2.3014 | 7.8327 | Porphyric granite | × | | | |
| DZ5a | 1 | 2.3014 | 7.8327 | Porphyric granite | × | × | | |
| DZ5b | 1 | 2.6471 | 8.2809 | Porphyric granite | × | | | |
| DZ6a | 1 | 2.6026 | 8.7477 | Porphyric granite | × | | | |
| DZ6b | 1 | 2.6026 | 8.7477 | Porphyric granite | × | | | |
| DZ7 | 1 | 2.6026 | 8.7477 | Porphyric granite | × | | | |
| DZ8 | 1 | 1.8906 | 8.4199 | Porphyric granite | × | | | |
| DZ9 | 1 | 1.8906 | 8.4199 | Porphyric granite | × | | | × |
| GLA1 | 1 | 1.8906 | 8.4199 | Migmatitic gneiss with biotite and amphibole | × | × | | |
| GLA2 | 1 | 1.8906 | 8.4199 | Porphyric granite | × | × | | |
| OU1 | 2 | 2.0069 | 7.7674 | Porphyric granite | × | × | × | |
| OU2 | 2 | 2.0439 | 7.7853 | Porphyric granite | × | | | |
| Ou3a | 2 | 2.1209 | 7.6808 | Porphyric granite | × | | | |
| Ou3b | 2 | 2.0969 | 7.8153 | Porphyric granite | × | | | |
| SVL1 | 1 | 2.1913 | 7.779 | Biotite granite | × | × | | |
| SVL2 | 1 | 2.1913 | 7.779 | Biotite granite | × | × | | |
| SVL3 | 1 | 2.2233 | 7.8338 | Biotite granite | × | | | × |

### 2.3. Hydrogeology

A shallow aquifer is developed in the weathered regolith layer and overlies a deep discontinuous aquifer located in the fractured bedrock (Boukari, 1982). The aquifer yield depends mostly on two parameters: thickness and effective porosity of the regolith on the one hand and the fracture density in the bedrock on the other hand. The fractured aquifers are the most productive and most used for water supply via boreholes equipped with hand pumps. The fractured aquifers are characterized by very low effective porosity values, on the order of 0.1–0.2% only. The transmissivity values depend greatly on the frequency and width of the fractures. Regolith aquifers are less productive for sustainable use, especially during the dry season, because most boreholes and wells drilled in this layer dry up. These aquifers are usually exploited through traditional open and large-diameter wells. The regolith aquifers have low permeability ($1 \times 10^{-7}$ to $9 \times 10^{-7}$ m/s), with effective porosity ranging between 2 and 5%, depending on the bedrock. As the communication between the two main groundwater reservoirs is well developed, they can be considered as a single aquifer system in which the regolith layer primarily acts as a storage region and the fractured zone as a transmissive one. Transmissivity values generally decrease from the regolith layer to the fractured zone (Boukari, 1982). Guihéneuf et al. (2014) have shown that in the crystalline aquifer, during high groundwater level conditions, the saprolite-granite interface controls groundwater flow at the watershed scale. In contrast, when groundwater levels are lower than this interface, hydrological compartmentalization appears, due to a decrease in the number of transmissive fractures with depth, which decreases connectivity with depth. Subsequently, the terms "shallow reservoir" and "deep reservoir" will be used for the regolith aquifer and the fractured aquifers, respectively.

### 2.4. Hydrogeochemistry and water quality in Central Benin

Our previous hydrogeochemical investigations in the area have revealed that groundwaters are largely of Ca–$HCO_3$ type, followed by Ca–Mg–Cl type (Tossou, 2016; Tossou et al., 2017). Groundwaters from the shallow aquifer appear to be more mineralized than those from the deep aquifer due to the anthropogenic contribution of wastewater effluents containing significant quantities of chemical compounds, such as$NO_3^-; Cl^-; SO_4^{2-}$, as well as the evapotranspiration effects, which tend to concentrate the dissolved compounds. Groundwaters in the southern part (Dassa-Zoumé and surroundings) have higher fluoride concentrations (3 mg/L on the average) than those from the northern part of the studied area (Bantè or Ouessè). In the north-western part (Bantè and surrroundings), fluoride concentrations are very low, generally below the WHO guidelines (1.5 mg/L). Additionally, surface water samples from rivers in the region show very low fluoride concentrations (max. 0.57 mg/L) ((Tossou et al., 2017).

Investigations have also shown that the groundwater mineralization is mainly controlled by water-rock interactions, in particular by the

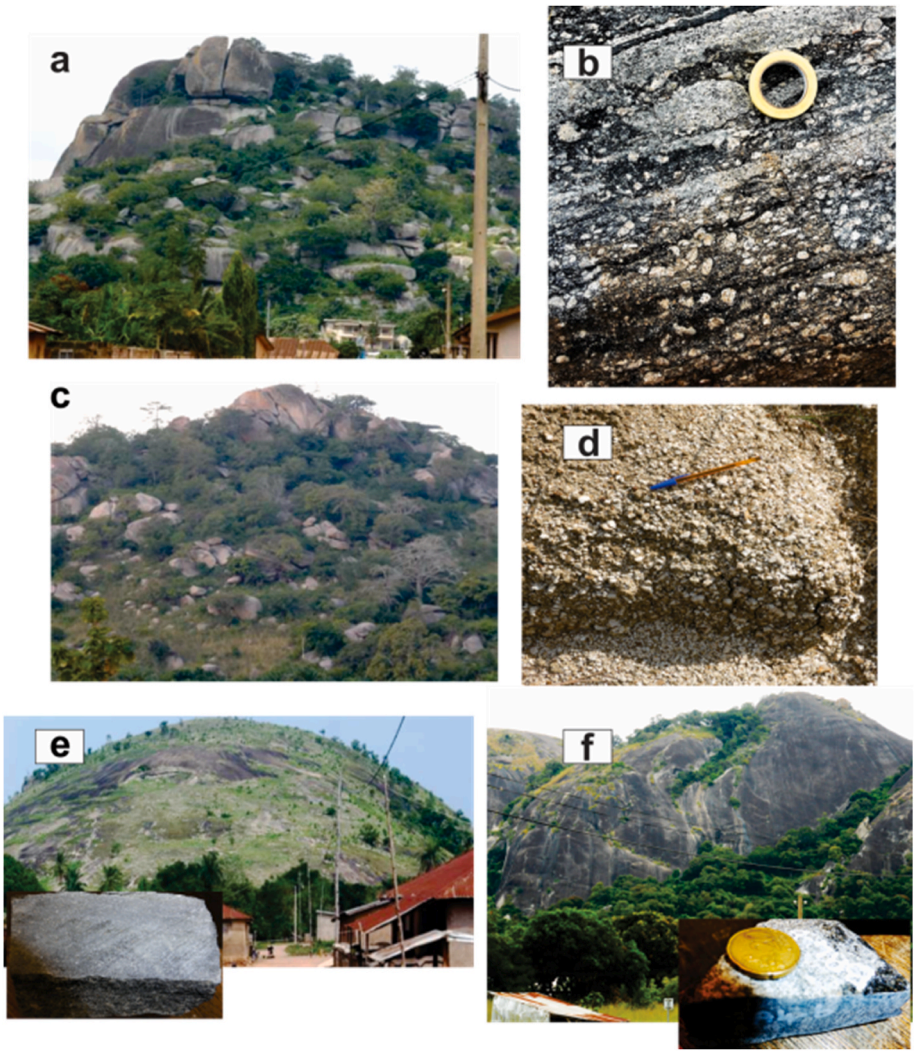


**Fig. 3.** Various morphology and texture of outcrops in the area. (a) and (c) granitic plutons with fractures closed to Dassa region (IZ1); (b) close-up of potassium feldspar porphyry from (a); (d) Clay from the incomplete alteration of the granite porphyry pluton of Soclogbo (IZ1); (e) and (f) fine grained compact hill closed to Gogoro, Ouessè (IZ2) and Bantè (IZ3).

hydrolysis of silicate minerals and fluoride has a geogenic origin related to the hydrolysis of fluorine-bearing minerals such as micas, amphiboles, fluorite (Tossou, 2016; Tossou et al., 2017).

## 3. Materials and methods

### 3.1. Field observations and rock samples collection

The rock samples were taken from three sites that were selected based on previous hydrogeochemical characterizations (Tossou et al., 2016). These sites are referred to as "Investigation Zone (Inv. Zone or IZ)" and shown in Fig. 2.

**Investigation Zone 1 (IZ1)** is located in the southern part of the region (Dassa-Zoumé and surroundings) and is characterized by the highest mineralized waters and fluoride concentrations (up to 7 mg/L). Twenty-four (24) rock samples were taken from various dominant rock facies (granites, gneiss, migmatite, volcanite) in this region.

**Investigation Zone 2 (IZ2)** is in the north-eastern sector of the department with less mineralized groundwater compared to Z1. Nevertheless, several groundwater samples show high fluoride concentrations (up to 3 mg/L). Four rock samples were collected in this region.

**Investigation Zone 3 (IZ3)** is in the north-western sector. Groundwater mineralization is similar to that observed in IZ2. This zone is characterized by rather low fluoride concentrations in groundwater (max 0.6 mg/L), always below the WHO standard for safety. Seven rock samples were collected in this area.

A total of 35 samples were collected. Most of them (34 samples) were taken from fresh and unweathered outcrops except sample DZ14 in IZ1 that was collected at a 10 m depth in a drilled well. This sample shows some degree of alteration and is friable (Table 2).

### 3.2. Analytical methods and data interpretation tools

#### 3.2.1. Samples analysis methods

A thin section was made for each sample on fresh specimens at the Laboratory of Petrology, Geochemistry and Petrophysics (University of Liège). The thin sections were subsequently analyzed under optical polarizing microscope in order to identify the minerals and their proportions. Mineral proportions were estimated semi-quantitatively using X-ray diffraction on rock powders at the Laboratory of Clays, Geochemistry and Sedimentary Environments, AGEs (University of Liège). With this method, the proportions of accessory phases (below 5%) such as fluorite and apatite, that may contain large proportions of fluorine, could not be quantified. Indeed, they were estimated with the point counting method on thin sections using an automatic digital PELCON point counter (Type NF EN 932-3). This manipulation was

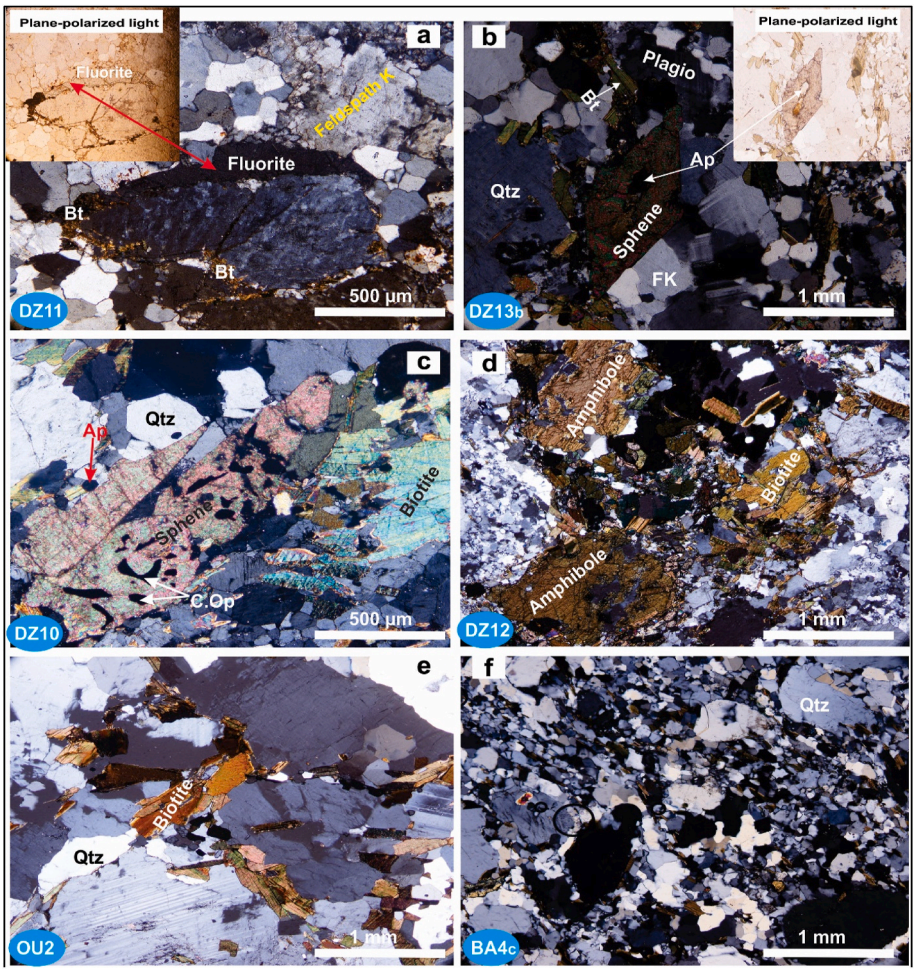


**Fig. 4.** Microphotographs of thin section of (a) alkali granite of Fita (IZ1); (b), (c) and (d) porphyric granite of Dassa-Zoumé (IZ1); (e) Fine grained granite, Gogoro-Ouessè (IZ2) and (f) fine grained and migmatitic gneiss, Bantè (IZ3). ***Bt:*** *Biotite;* ***Ap:*** *Apatite;* ***Qtz:*** *Quartz;* ***Plagio:*** *plagioclase;* ***FK:*** *Potassium feldspar;* ***C. Op:*** *Opaque minerals.* Sample numbers are given in the blue filled oval on each photograph.

carried out on ten thin sections, mainly on the samples with the higher fluorine concentration. A mechanical slider was moved in steps of 1 mm in X and Y directions producing 500 points per thin section. Mass fractions were determined using an average density of 2.5 g/cm$^3$.

Major elements and fluorine concentrations (wt. %) in the minerals were measured using the Cameca SX-100 electron microprobe at Blaise Pascal University (Clermont-Ferrand, France) on a selection of ten polished thin sections (6 in IZ1, 2 in IZ2 and 2 in IZ3) which representated the different geological formations. The chemical composition of some of the fluorinated minerals together with their structural formulas are presented in the Supplementary Material. Six samples were also examined using Scanning Electron Microscopy at the Functional and Evolutionary Morphology Laboratory (University of Liège) on polished sections for mapping of various elements and identification of some minerals that might not have been recognized by optical microscopy. Major elements ($SiO_2$, $Al_2O_3$, CaO, MgO, $K_2O$, $Na_2O$, MnO, $P2O_5$, $Fe_2O_3$ and $TiO_2$) and some trace elements (Co, Cu, Ga, Nb, Ni, Pb, Rb, Sr, Th, U, Y, Zn, Zr) were measured by X-ray fluorescence (ARL 9400 XP wavelength-dispersive (WD)-XRF spectrometer) on fused glass discs and pressed powdered pellets at the Laboratory of Petrology, Geochemistry and Petrophysics (University of Liège).

The determination of fluorine concentration in the whole rock samples was performed by potentiometry with a specific electrode at the Petrochemical and Geochemical Research Center (CRPG), Nancy, France.

### 3.2.2. Data interpretation tools

Binary graphs to multivariate statistics, were used to explore the mineral and geochemical data. Multivariate analysis tools, mainly the Self Organizing Map (SOM) method (Kohonen, 1982, 1998), were used to highlight the contribution of each fluorine-bearing minerals to the total fluorine of the rock. The SOM method allows projecting multidimensional data on a two-dimensional grid to capture complex (non linear) relationships between variables (Peters et al., 2007). The visual comparison of resulting individual component planes allows for the identification of statistical relationships (further called correlations) between the analyzed variables and to separate the dataset into different groups of similar geochemical features. Here, the SOM method has helped to identify clusters (samples) of similar geochemical and mineralogical characteristics and to point out correlations between the different variables that characterize the samples. For the present study, the "SOM toolbox" interface for Matlab (2012 version) was used for the analysis.

Hierarchical Ascendant Classification (HAC) was also used as a complement to the SOM method in order to corroborate results of classification and individuals clustering. If HAC is frequently used in geochemical studies (Chery et al., 2000, 2003; Ladouche et al., 2004; Brinis and Boudoukha, 2011), the SOM method is less known but it has found frequent applications recently in the field of the geosciences (Ultsch et al., 1989; Giraudel et al., 2001; Ultsh et al., 2005; Kalteh et al., 2007; Kamagaté, 2010; Kyung-Jin et al., 2019; Ge et al., 2020; Kim et al., 2020).

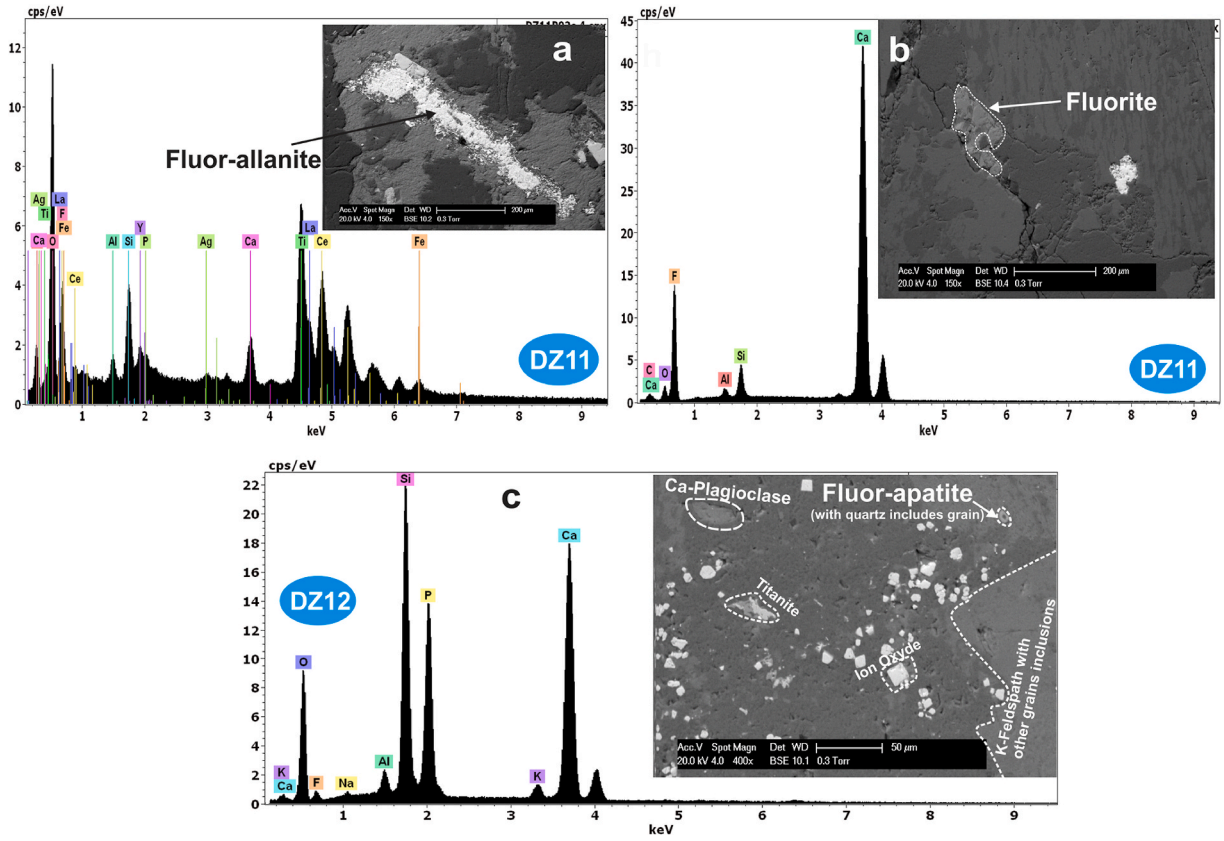


**Fig. 5.** Scans and chemical spectra obtained by Scanning Electron Microscopy (SEM) on fluorine-bearing from rock samples of IZ1. (a) Fluor-allanite of samples DZ11; (b) Fluorite of sample DZ11; (c) Fluor-apatite including silica in sample DZ12.

## 4. Results

### 4.1. Field and petrographic data

We will first describe the different geological facies that were recognized during our field campaigns. From one investigation zone to another, large variability and heterogeneity can be observed when considering the morphology and the grain-size of the geological formations (Fig. 3). The IZ1 (Dassa-Zoumé and vicinity) is characterized by long chain hills with heavily fractured outcrops (Fig. 3a–d). By contrast, in IZ2 and IZ3, there are fewer outcrops and they are often present as domes with low altitude surfaces (Fig. 3e and f). Moreover, in IZ1, the outcrops usually display porphyritic facies whereas in the other zones (IZ2 and IZ3), rocks are finer grained. Within each IZ, textural heterogeneity is also observed. In the porphyry granite of Dassa, the granulometry of the potassic feldspar increases towards the eastern part of the massif (Soclogbo, Gbaffo and Minifi region). In this part, the outcrops contain centimetric crystals of feldspar and there are high amount of arena and clay minerals (as shown by Fig. 3c and d from outcrops at Awaya, in the region of Awaya-Gbaffo). Such zonal differentiation and the effects of chemical alteration of the outcrops are minimal in IZ2 and IZ3.

The examination of the thin sections under optical microscopy (Fig. 4 a, **b, c, d, e, f)** together with the analysis by scanning electron microcopy (Fig. 5 a, **b, c)** revealed that the most abundant minerals are quartz, plagioclase, potassic feldspar (orthoclase, microcline) and biotite. The accessory minerals that were observed are hornblende, titanite, fluorite, apatite (locally included in other minerals such as biotite and plagioclase), garnet, olivine, pyroxene, zircon, opaque minerals and fluor-allanite. Previous studies by Boussari (1975), Boukari (1982), Biggiogero (1988) ***and*** Adissin Glodji et al. (2014), Adissin Glodji (2012) pointed out the presence of such minerals in the area. In IZ1 (southern part of the region), Boussari (1975) particularly emphasized the occurrence of fluorite, locally included in biotite.

Samples from the IZ3 display less mineralogical diversity than those of IZ1 and IZ2. Most importantly, fluorite is not observed and the abundance of biotite is low. The thin section analysis also confirms that in IZ3 (and in IZ2), medium to fine grained textures prevail, while porphyritic texture is dominant in IZ1 (Fig. 4).

Among the minerals recognized in thin sections, several contain fluoride. These include fluorite, biotite, muscovite, amphiboles, chlorite, titanite and apatite. These minerals are more abundant in samples of IZ1 and IZ2 than in IZ3.

### 4.2. Mineral composition and proportions

X-ray diffraction performed on whole rock powders indicate that the most frequent minerals are quartz, micas (mainly biotite), plagioclase and potassium feldspar. Pyroxenes, amphiboles and chlorite were also identified in some of the samples. The mineral composition (wt. %) of each sample is presented in Table 3.

Electron microprobe and scanning electron microscopy analysis also reveal the presence of epidote, ilmenite, fluorite and fluorine-allanite that could not be identified with certainty under the optical microscope.

The proportions of most accessory minerals observed in thin sections could not be quantified by XRD. As indicated above (section 3.2.1), this was done using the point counting method. The results are presented in Table 4. The proportions of fluorine-rich minerals (apatite, fluorite and muscovite) are all relatively low (<1%).

Fig. 6 shows spatial distribution of the mineral compositions in the study area. According to the investigations zones (IZ), biotite, anorthite, titanite and microcline are more abundant in IZ1 than in IZ2 and IZ3. In contrast, samples from IZ2 and IZ3 contain more quartz and orthoclase is clearly dominant in IZ3.

**Table 3**
Mineral proportions by DRX (wt. %) and concentrations of major elements (wt. %) and fluorine (ppm) in rocks samples.

| Samples | BA1 | BA2 | BA3 | BA4a | BA4b | BA4c | BA4d | DZ10 | DZ11 | DZ12 | DZ13a | DZ13b | DZ14 | DZ1a | DZ1b | DZ2 | DZ3 | DZ4a |
|---|---|---|---|---|---|---|---|---|---|---|---|---|---|---|---|---|---|---|
| **Quartz** | 39.00 | 30.00 | 33.00 | 37.00 | 39.00 | 40.00 | 35.00 | 33.00 | 34.00 | 24.00 | 32.00 | 32.00 | 0.00 | 38.00 | 31.50 | 22.50 | 34.00 | 28.00 |
| **Orthoclase** | 5.50 | 6.00 | 4.00 | 5.00 | 3.00 | 3.00 | 6.00 | 2.00 | 3.00 | 0.50 | 1.00 | 1.00 | 0.00 | 1.50 | 3.00 | 3.00 | 1.00 | 4.00 |
| **Albite** | 25.00 | 10.00 | 21.00 | 29.50 | 29.00 | 31.00 | 23.00 | 24.00 | 29.00 | 53.00 | 18.50 | 20.00 | 0.00 | 20.00 | 21.50 | 21.50 | 22.50 | 19.00 |
| **Anorthite** | 8.00 | 23.00 | 3.00 | 6.00 | 6.00 | 6.00 | 2.00 | 15.00 | 6.00 | 2.00 | 6.00 | 5.00 | 6.00 | 2.00 | 6.00 | 6.50 | 2.50 | 10.50 |
| **Biotite** | 5.00 | 20.00 | 1.00 | 5.00 | 5.00 | 6.00 | 6.00 | 7.50 | 2.00 | 0.50 | 7.50 | 8.00 | 0.00 | 1.50 | 12.50 | 9.00 | 6.00 | 14.50 |
| **Titanite** | 0.00 | 2.00 | 0.00 | 2.50 | 1.50 | 1.50 | 2.00 | 2.50 | 1.00 | 1.00 | 2.00 | 2.00 | 0.50 | 0.50 | 2.00 | 2.00 | 1.50 | 2.00 |
| **Microcline** | 17.00 | 6.00 | 38.00 | 14.50 | 14.00 | 12.00 | 20.00 | 12.00 | 25.00 | 19.00 | 31.00 | 30.00 | 1.00 | 36.50 | 22.50 | 32.00 | 30.50 | 18.50 |
| **Amphibole** | 0.50 | 1.50 | 0.00 | 0.50 | 2.50 | 0.50 | 5.00 | 0.00 | 0.00 | 0.00 | 0.00 | 0.00 | 88.50 | 0.00 | 1.00 | 3.50 | 0.00 | 3.50 |
| **Pyroxene** | 0.00 | 1.50 | 0.00 | 0.00 | 0.00 | 0.00 | 0.00 | 0.00 | 0.00 | 0.00 | 0.00 | 0.00 | 0.00 | 0.00 | 0.00 | 0.00 | 0.00 | 0.00 |
| **Chlorite** | 0.00 | 0.00 | 0.00 | 0.00 | 0.00 | 0.00 | 1.00 | 4.00 | 0.00 | 0.00 | 2.00 | 2.00 | 4.00 | 0.00 | 0.00 | 0.00 | 2.00 | 0.00 |
| **Total** | **100.0** | **100.0** | **100.0** | **100.0** | **100.0** | **100.0** | **100.0** | **100.0** | **100.0** | **100.0** | **100.0** | **100.0** | **100.0** | **100.0** | **100.0** | **100.0** | **100.0** | **100.0** |
| **$Al_2O_3$** | 14.86 | 15.72 | 14.22 | 14.98 | 14.86 | 15.08 | 12.96 | 15.57 | 12.47 | 14.11 | 13.80 | 13.92 | 5.28 | 12.72 | 15.35 | 15.78 | 13.80 | 15.37 |
| **CaO** | 2.01 | 4.33 | 0.94 | 2.29 | 2.35 | 2.38 | 2.29 | 3.21 | 0.69 | 0.67 | 2.09 | 2.02 | 13.04 | 1.03 | 3.23 | 2.49 | 1.54 | 4.19 |
| **$Fe_2O_3$** | 1.33 | 7.84 | 0.64 | 1.55 | 1.80 | 1.77 | 5.61 | 2.72 | 1.69 | 3.59 | 3.74 | 3.66 | 10.66 | 0.73 | 4.77 | 4.97 | 3.25 | 5.92 |
| **$K_2O$** | 3.49 | 2.67 | 7.16 | 3.32 | 3.31 | 2.87 | 5.33 | 3.69 | 5.41 | 3.24 | 5.79 | 5.58 | 0.58 | 5.87 | 4.57 | 5.95 | 5.76 | 4.05 |
| **MgO** | 0.34 | 2.27 | 0.00 | 0.33 | 0.37 | 0.39 | 0.28 | 0.70 | 0.00 | 0.00 | 0.54 | 0.57 | 16.20 | 0.11 | 1.24 | 0.88 | 0.32 | 1.57 |
| **MnO** | 0.03 | 0.12 | 0.01 | 0.04 | 0.05 | 0.04 | 0.09 | 0.04 | 0.02 | 0.06 | 0.05 | 0.05 | 0.21 | 0.01 | 0.08 | 0.07 | 0.04 | 0.09 |
| **$Na_2O$** | 4.36 | 3.25 | 2.30 | 4.03 | 3.91 | 4.13 | 2.16 | 3.66 | 3.07 | 5.56 | 2.23 | 2.31 | 0.12 | 2.66 | 3.45 | 3.39 | 2.88 | 2.84 |
| **$P_2O_5$** | 0.05 | 0.43 | 0.11 | 0.03 | 0.02 | 0.03 | 0.17 | 0.13 | 0.00 | 0.00 | 0.19 | 0.19 | 0.03 | 0.05 | 0.31 | 0.23 | 0.11 | 0.33 |
| **$SiO_2$** | 72.38 | 62.01 | 72.69 | 70.91 | 71.20 | 71.87 | 69.25 | 66.62 | 74.61 | 70.59 | 69.64 | 70.08 | 51.35 | 75.25 | 65.92 | 63.84 | 71.72 | 63.21 |
| **$TiO_2$** | 0.19 | 1.22 | 0.06 | 0.22 | 0.23 | 0.23 | 0.73 | 0.55 | 0.17 | 0.35 | 0.61 | 0.55 | 0.56 | 0.13 | 0.86 | 0.79 | 0.38 | 1.09 |
| **LOI** | 0.38 | 0.73 | 0.29 | 0.04 | 0.57 | 0.36 | 0.13 | 0.52 | 0.70 | 0.40 | 0.42 | 0.46 | 3.18 | 0.43 | 0.62 | 0.68 | 0.91 | 0.39 |
| **Total** | **99.42** | **100.59** | **98.42** | **97.73** | **98.67** | **99.15** | **99.01** | **97.39** | **98.83** | **98.55** | **99.10** | **99.38** | **101.20** | **98.99** | **100.39** | **99.07** | **100.71** | **99.06** |
| **F (ppm)** | 350 | 970 | 210 | 380 | 390 | 400 | 410 | 1000 | 2900 | 100 | 2000 | 1800 | 500 | 290 | 2500 | 1200 | 1600 | 2100 |

| Samples | DZ4b | DZ5a | DZ5b | DZ6a | DZ6b | DZ7 | DZ8 | DZ9 | GLA1 | GLA2 | OU1 | OU2 | Ou3a | Ou3b | SVL1 | SVL2 | SVL3 |
|---|---|---|---|---|---|---|---|---|---|---|---|---|---|---|---|---|---|
| **Quartz** | 34.00 | 30.50 | 25.50 | 34.00 | 31.50 | 22.50 | 25.00 | 33.00 | 40.50 | 33.00 | 40.00 | 38.00 | 30.00 | 44.50 | 15.00 | 34.50 | 18.50 |
| **Orthoclase** | 1.00 | 1.50 | 4.00 | 2.00 | 2.00 | 1.50 | 2.00 | 2.50 | 2.50 | 1.50 | 1.50 | 2.00 | 2.00 | 1.50 | 0.00 | 1.00 | 1.50 |
| **Albite** | 19.00 | 19.50 | 19.00 | 14.50 | 13.00 | 19.50 | 25.00 | 19.00 | 32.50 | 27.00 | 25.00 | 23.00 | 25.00 | 23.00 | 33.00 | 26.50 | 26.00 |
| **Anorthite** | 3.00 | 14.50 | 17.00 | 9.00 | 9.00 | 10.00 | 8.00 | 13.50 | 2.00 | 2.50 | 2.50 | 2.00 | 2.50 | 2.00 | 1.00 | 1.00 | 2.00 |
| **Biotite** | 7.00 | 20.50 | 24.00 | 10.00 | 12.50 | 10.00 | 11.00 | 13.00 | 0.50 | 10.50 | 2.50 | 6.00 | 14.00 | 6.00 | 17.00 | 5.00 | 14.50 |
| **Titanite** | 1.50 | 2.00 | 2.50 | 1.50 | 2.00 | 2.00 | 3.00 | 3.00 | 2.00 | 2.50 | 1.00 | 1.50 | 3.00 | 1.00 | 2.50 | 1.00 | 2.00 |
| **Microcline** | 32.50 | 11.50 | 8.00 | 29.00 | 30.00 | 30.50 | 22.50 | 13.50 | 20.00 | 23.00 | 27.00 | 26.00 | 17.50 | 20.00 | 10.00 | 29.00 | 29.00 |
| **Amphibole** | 0.00 | 0.00 | 0.00 | 0.00 | 0.00 | 4.00 | 3.50 | 2.50 | 0.00 | 0.00 | 0.00 | 0.00 | 4.00 | 0.00 | 19.50 | 0.00 | 6.50 |
| **Pyroxene** | 0.00 | 0.00 | 0.00 | 0.00 | 0.00 | 0.00 | 0.00 | 0.00 | 0.00 | 0.00 | 0.00 | 0.00 | 0.00 | 0.00 | 0.00 | 0.00 | 0.00 |
| **Chlorite** | 2.00 | 0.00 | 0.00 | 0.00 | 0.00 | 0.00 | 0.00 | 0.00 | 0.00 | 0.00 | 0.50 | 1.50 | 2.00 | 2.00 | 2.00 | 2.00 | 0.00 |
| **Total** | **100.0** | **100.0** | **100.0** | **100.0** | **100.0** | **100.0** | **100.0** | **100.0** | **100.0** | **100.0** | **100.0** | **100.0** | **100.0** | **100.0** | **100.0** | **100.0** | **100.0** |
| **$Al_2O_3$** | 13.65 | 15.62 | 15.81 | 13.48 | 13.80 | 15.36 | 15.05 | 15.34 | 13.79 | 14.47 | 13.50 | 13.71 | 15.32 | 13.52 | 16.77 | 14.03 | 16.77 |
| **CaO** | 1.43 | 4.27 | 4.34 | 1.73 | 1.80 | 3.32 | 3.53 | 4.08 | 0.71 | 2.32 | 1.30 | 1.91 | 3.92 | 1.71 | 6.31 | 1.39 | 4.80 |
| **$Fe_2O_3$** | 3.30 | 6.43 | 5.92 | 3.37 | 3.49 | 5.58 | 6.99 | 5.92 | 0.67 | 4.75 | 1.78 | 3.39 | 5.75 | 2.84 | 8.38 | 2.39 | 6.07 |
| **$K_2O$** | 6.12 | 3.54 | 3.62 | 6.03 | 6.12 | 5.49 | 4.75 | 4.06 | 5.32 | 5.56 | 5.03 | 5.42 | 4.22 | 3.80 | 1.72 | 5.10 | 4.67 |
| **MgO** | 0.27 | 2.35 | 2.24 | 0.35 | 0.41 | 0.93 | 0.94 | 1.54 | 0.04 | 0.75 | 0.29 | 0.45 | 1.44 | 0.35 | 3.73 | 0.26 | 2.12 |
| **MnO** | 0.05 | 0.10 | 0.07 | 0.04 | 0.04 | 0.08 | 0.11 | 0.09 | 0.02 | 0.07 | 0.03 | 0.05 | 0.08 | 0.05 | 0.13 | 0.05 | 0.12 |
| **$Na_2O$** | 2.03 | 2.95 | 3.05 | 1.85 | 1.87 | 2.73 | 3.04 | 2.90 | 3.45 | 3.06 | 3.19 | 2.28 | 2.83 | 2.86 | 4.40 | 3.11 | 3.00 |
| **$P_2O_5$** | 0.09 | 0.30 | 0.34 | 0.16 | 0.15 | 0.21 | 0.25 | 0.31 | 0.00 | 0.29 | 0.09 | 0.14 | 0.31 | 0.11 | 0.45 | 0.07 | 0.33 |
| **$SiO_2$** | 71.37 | 62.09 | 62.03 | 71.20 | 70.16 | 63.26 | 63.02 | 63.49 | 75.69 | 67.38 | 73.53 | 70.56 | 63.41 | 72.81 | 56.44 | 72.14 | 60.47 |
| **$TiO_2$** | 0.40 | 1.10 | 1.20 | 0.53 | 0.51 | 0.90 | 1.05 | 1.08 | 0.08 | 0.78 | 0.28 | 0.55 | 1.11 | 0.37 | 1.27 | 0.33 | 0.66 |
| **LOI** | 0.43 | 0.55 | 0.63 | 0.49 | 0.40 | 0.40 | 0.31 | 0.42 | 0.92 | 0.73 | 0.64 | 0.37 | 0.56 | 0.43 | 1.20 | 0.38 | 0.60 |
| **Total** | **99.15** | **99.30** | **99.25** | **99.24** | **98.75** | **98.26** | **99.04** | **99.23** | **100.69** | **100.16** | **99.67** | **98.82** | **98.94** | **98.84** | **100.81** | **99.24** | **99.59** |

**Table 4**
Mineral proportions (wt. %) estimated by points counting.

| Samples. | BA1 | BA2 | DZ11 | DZ13a | DZ13b | DZ1a | DZ3 | DZ9 | GLA2 | OU2 |
|---|---|---|---|---|---|---|---|---|---|---|
| Quartz | 39.79 | 33.40 | 34.85 | 30.71 | 30.78 | 39.79 | 32.11 | 33.20 | 32.05 | 33.69 |
| Plagioclase | 33.33 | 30.01 | 35.05 | 24.45 | 24.45 | 21.22 | 24.15 | 32.66 | 31.51 | 25.37 |
| Potassium Feldspath | 19.83 | 6.51 | 25.03 | 29.51 | 30.11 | 35.81 | 31.44 | 13.55 | 22.12 | 27.36 |
| Chlorite | 0.00 | 0.00 | 0.00 | 2.27 | 2.00 | 0.00 | 2.14 | 0.00 | 0.00 | 1.46 |
| Oxyde | 0.47 | 0.53 | 0.27 | 0.67 | 0.47 | 0.20 | 0.13 | 0.40 | 0.33 | 1.40 |
| Sphene | 0.00 | 2.52 | 1.00 | 2.13 | 2.27 | 0.60 | 1.54 | 3.02 | 2.47 | 1.66 |
| Biotite | 5.06 | 21.25 | 2.00 | 7.66 | 7.99 | 1.66 | 6.56 | 13.08 | 10.46 | 6.99 |
| Muscovite | 0.40 | 0.80 | 0.40 | 1.00 | 0.47 | 0.00 | 0.27 | 0.67 | 0.60 | 0.33 |
| Amphibole | 0.60 | 2.52 | 0.00 | 0.00 | 0.00 | 0.00 | 0.00 | 2.48 | 0.00 | 0.00 |
| Zircon | 0.00 | 0.27 | 0.40 | 0.73 | 0.60 | 0.33 | 1.00 | 0.54 | 0.20 | 0.80 |
| Pyroxene | 0.53 | 2.12 | 0.33 | 0.20 | 0.47 | 0.40 | 0.54 | 0.27 | 0.07 | 0.53 |
| Apatite | 0.00 | 0.07 | 0.13 | 0.33 | 0.27 | 0.00 | 0.13 | 0.13 | 0.20 | 0.27 |
| Fluorite | 0.00 | 0.00 | 0.53 | 0.33 | 0.13 | 0.00 | 0.00 | 0.00 | 0.00 | 0.13 |
| Total (%) | **100** | **99.9** | **99.3** | **99.33** | **99.6** | **100** | **99.9** | **99.9** | **99.8** | **99.6** |

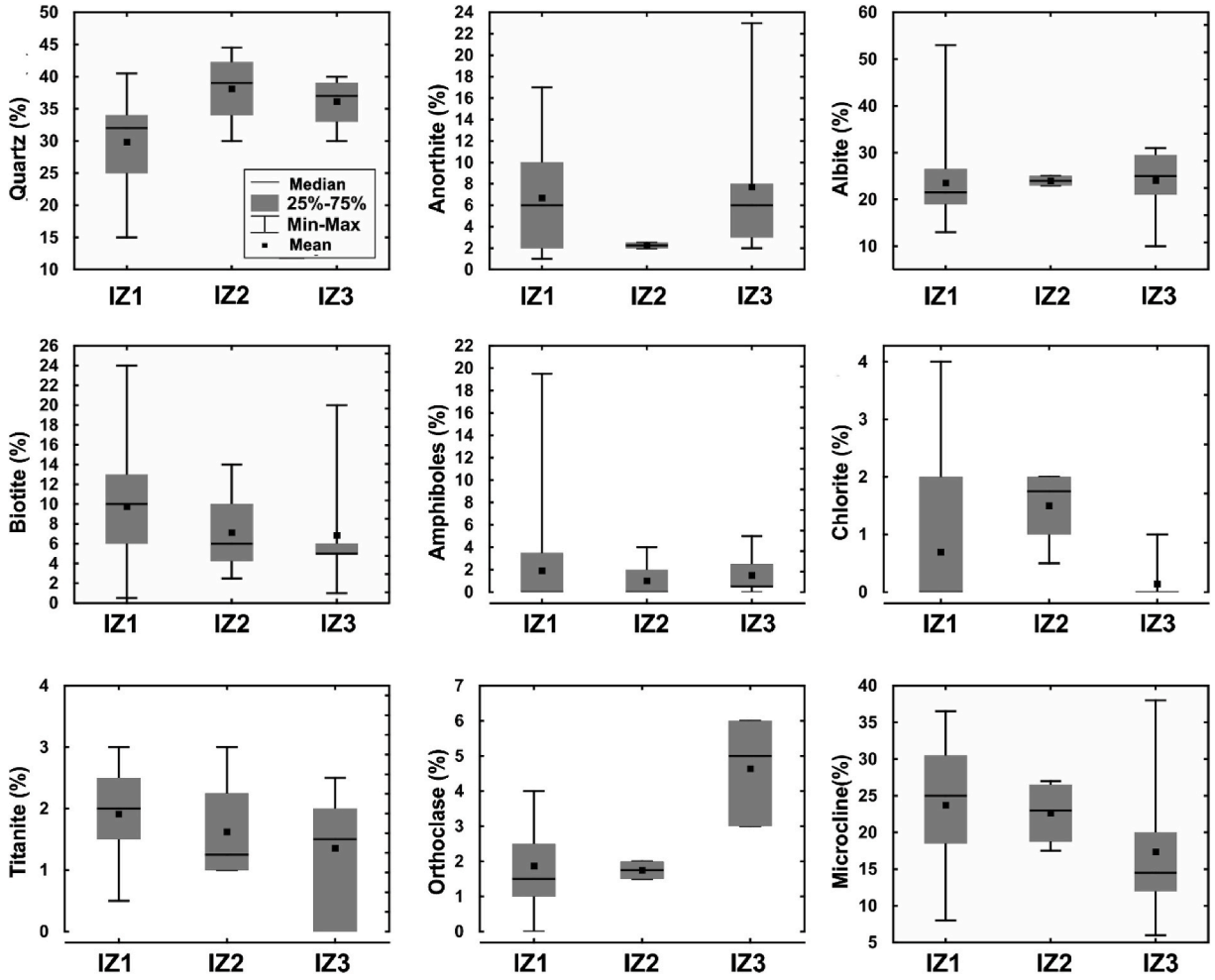


**Fig. 6.** Minerals proportions (wt. %) by X-Ray Diffraction (XRD) according to Investigation Zone (IZ).

### *4.3. Geochemistry*

Fig. 7 presents the variations of fluorine concentration (ppm) and major elements (wt. %) in each investigation zone. The plots show some spatial variability in the distribution of these elements.MgO, $K_2O$, MnO, $P_2O_5$, $Fe_2O_3$ and $TiO_2$ display their highest and lowest concentrations respectively in IZ1 and IZ3. The opposite situation is observed for $SiO_2$, $Al_2O_3$ and $Na_2O$ that are higher in IZ3 and lower in IZ1. CaO concentration is similar in the three IZ with slightly higher concentrations in IZ1. These observations are consistent with the variable proportions of minerals.

The concentration of fluorine ranges from 60 to 2900 ppm with an average of 1171 ppm. Samples of IZ1 have the greatest concentration of fluorine followed by those of IZ2 and then IZ3.

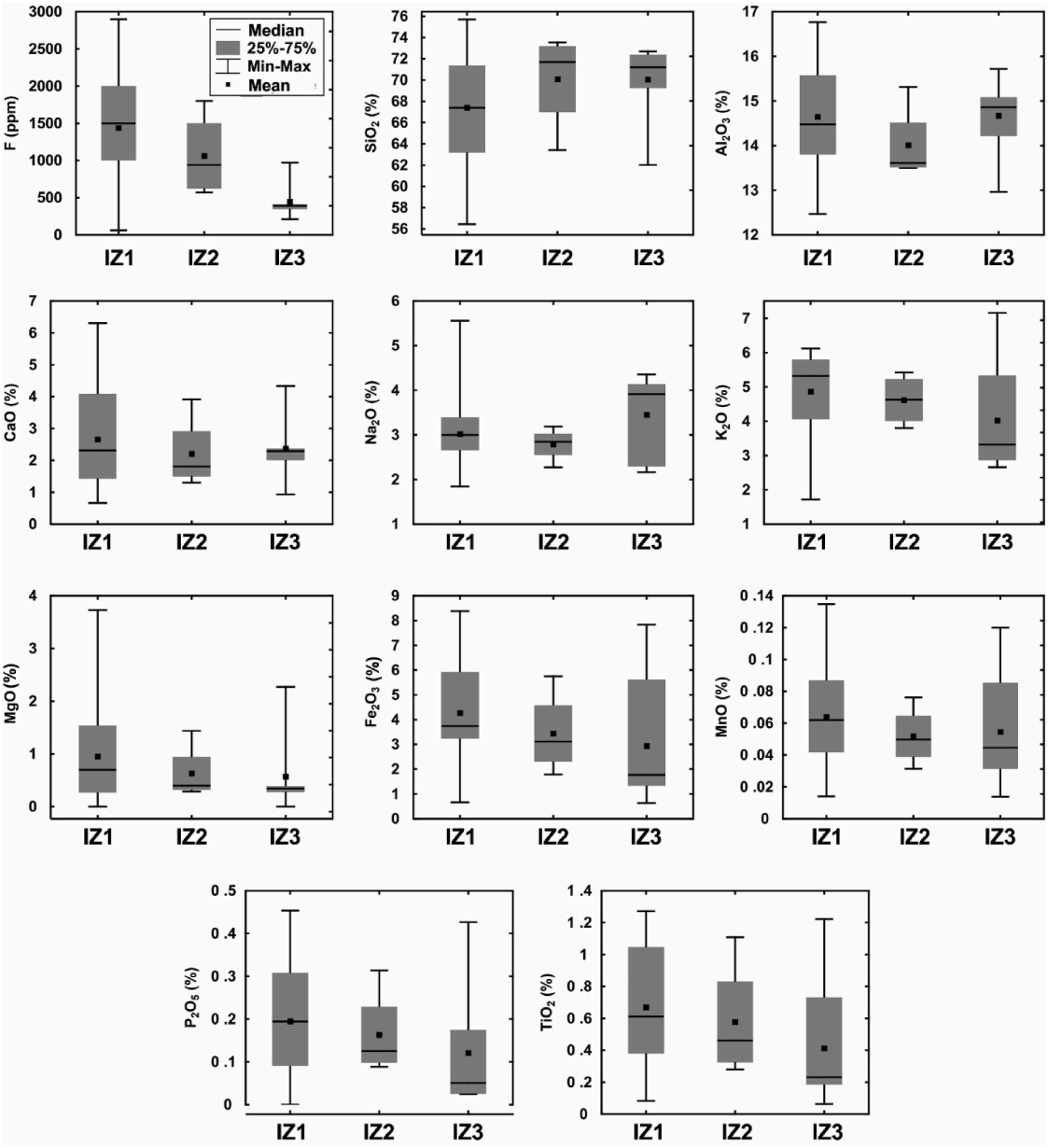


**Fig. 7.** Fluorine concentration (ppm) and major elements (wt. %) in whole rock according to Investigation Zone (IZ).

## 5. Discussion

### *5.1. Petrography and mineralogy impact on the spatial differentiation of groundwater mineralization and its fluoride concentrations in the region*

The petrographic analysis shows that the geological formations in the study area exhibit strong spatial variability in their textures and mineralogy. In IZ1 and especially in the areas closed to the Dassa-Zoumé pluton, rock materials show large grain sizes with clear indications of advanced physical and chemical weathering. In particular, the outcrops show fractures and large quantities of clay minerals are observed around the foothills. In contrast, outcrops in IZ2 and IZ3 display fine grain and are less fractured. This most probably explains the spatial variations of groundwater hydrogeochemistry in the region since the most mineralized groundwater are in IZ1 and especially in the areas closed to the Dassa-Zoumé pluton as previously stated by Tossou et al. (2017). Indeed, Hoareau et al. (2005) reported that the differentiation of rocks and the proportion of large grains in the rock play an important role in controlling the composition of weathering solutions. According to Rondeau (1960) and Dutreuil (1979), porphyric formations are more easily affected by physical disaggregation phenomena and in this way are most subject to chemical weathering, making the groundwater more mineralized.

In terms of the spatial distribution of the mineral compositions (according to the investigations zones – IZ) (Fig. 6), biotite, anorthite, titanite and microcline are more abundant in IZ1 than in IZ2 and IZ3. In contrast, samples from IZ2 and IZ3 contain more quartz with high dominance of orthoclase in IZ3. According to Goldich's weathering series (Goldich, 1938), the most resistant minerals to chemical weathering are quartz or orthoclase and these show higher proportions in IZ2 and IZ3. Thus, chemical weathering of rocks in these areas will be less intense than elsewhere. This probably explains the lowest water mineralization recorded by Tossou et al. (2017) in these investigation zones compared to IZ1.

The recorded concentrations of fluorine in rock samples in the study area (60–2900 ppm with an average of 1171 ppm) compare very well with those observed worldwide in areas where groundwater shows anomalously high concentrations of fluoride (Apambire et al., 1997;

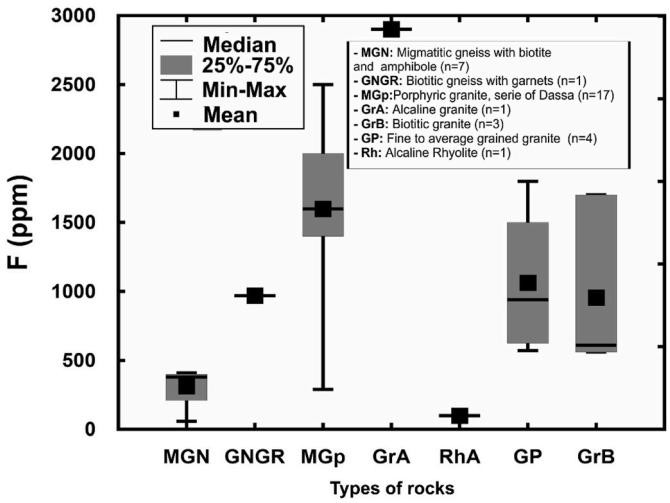


**Fig. 8.** Fluorine concentration (ppm) of rocks samples according to their lithology.

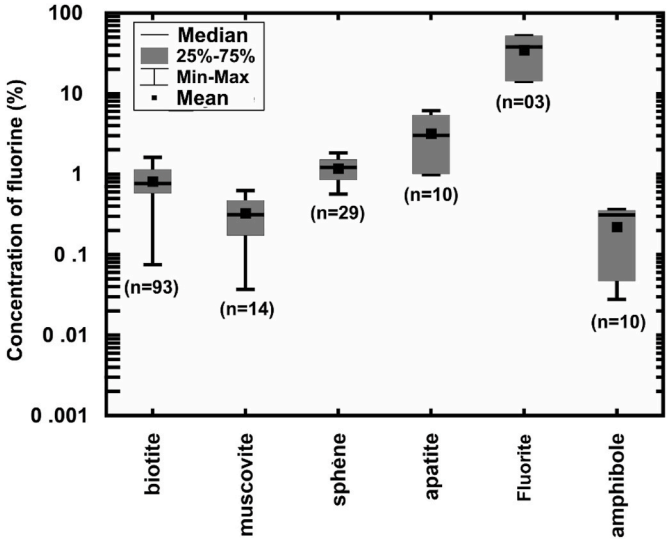


**Fig. 9.** Fluorine concentration of the different fluorine-bearing minerals measured by electron microprobe.

Gunnar et al., 2005; Abdelgawad et al., 2009; Maria et al., 2015; Hayes et al.,. 2017; Missi, and Atekwana, 2020).

The F concentration of the lithologies composing the bedrock largely varies as shown in Fig. 8. Granites, especially those located close to the Dassa-Zoumé region, have significant concentrations of fluorine (290–2900 ppm) whereas migmatites and gneiss appear to be poor in fluorine (Fig. 8). The highest fluorine concentration has been recorded in the alkali granite of Fita (sample DZ 11 = sample GrA on Fig. 8). This abundance of fluorine in IZ1 rocks compared to the other IZ, coupled with the high alterability of the rocks in IZ1 could well explain the high fluoride content in groundwater from IZ1 as reported by Tossou et al. (2017).

### 5.2. Main sources of F in the rocks

Electron microprobe and scanning electron microscope (SEM) analyses confirmed that several minerals, particularly in IZ1, contain fluorine in their structure: fluorite, apatite, biotite, titanite, amphibole and muscovite. In some minerals, such as chlorite, epidote and clays, fluorine was also detected but in very low quantity (generally less than 0.05 wt %) (Fig. 9 and Table 5).

### 5.3. Estimating the contribution of fluorine-bearing minerals to the total fluorine concentration of the rocks

#### 5.3.1. Assessing the relationship between fluorine and various minerals by multivariate analysis

The data used for the analysis consist of the mineralogical compositions and the geochemical of the samples. The mineral proportions (wt. %) that were used are those derived exclusively from the XRD data because point counting was performed on only 10 samples and data for some minerals such as fluorite and apatite were acquired in even fewer samples (3–5).

The results provided by the SOM analysis are presented in Fig. 10a and Fig. 11.

The aggregation plot for samples by the SOM method shows three main clusters/groups, G1 to G3 (Fig. 10a). Analysis by the Ascending Hierarchical Classification (AHC) approach corroborate the clustering results provided by the SOM approach, as shown in Fig. 10b.

The simultaneous analysis of the clusters chart and the component plane (correlations map) (Fig. 11) shows that Group 1 includes samples with the highest concentration of fluorine and includes most samples of IZ1 and some of IZ2. The samples of group 3 with the lowest concentrations of fluorine are mostly from the IZ3. In group 2 fluorine concentrations are intermediate between the other two groups.

Furthermore, from the analysis of component matrices (Fig. 11) between various parameters (fluorine concentration, proportions of

**Table 5**
Summary statistics of fluorine concentrations (wt. %) in fluorine-rich minerals. N: Number of samples; Med.: Median; Min.: Minimum; Max.: Maximum; P25: 25th percentile; P75: 75th percentile; SD: Standard Deviation.

| Mineral | N | Mean | Med. | Min. | Max. | P25 | P75 | SD |
|---|---|---|---|---|---|---|---|---|
| Fluorite | 3 | 34.84 | 38.03 | 14.30 | 52.19 | 14.30 | 52.19 | 19.14 |
| Apatite | 10 | 3.19 | 3.01 | 0.99 | 6.11 | 1.00 | 5.41 | 2.13 |
| Sphène | 29 | 1.18 | 1.21 | 0.56 | 1.84 | 0.85 | 1.51 | 0.38 |
| Biotite | 93 | 0.81 | 0.76 | 0.07 | 1.62 | 0.58 | 1.13 | 0.39 |
| Muscovite | 14 | 0.33 | 0.31 | 0.04 | 0.62 | 0.17 | 0.47 | 0.20 |
| Amphibole | 10 | 0.22 | 0.31 | 0.03 | 0.36 | 0.05 | 0.35 | 0.16 |
| Clay | 2 | 0.05 | 0.05 | 0.02 | 0.09 | 0.02 | 0.09 | 0.05 |
| Epidote | 2 | 0.03 | 0.03 | 0.01 | 0.04 | 0.01 | 0.04 | 0.02 |
| Chlorite | 2 | 0.01 | 0.01 | 0.01 | 0.01 | 0.01 | 0.01 | 0.00 |

The SEM also revealed the local presence of fluor-allanite (Fig. 5a) that contains 5.35 wt % of fluorine. Fluorite, in which fluorine is a major element (43.28 wt %), as well as fluor-apatite, were also identified by the SEM (Fig. 5b). In the latter, the highest proportion of fluorine measured by the SEM was 10.48 wt %, which is slightly higher than all the values obtained by the electron microprobe. In the samples of IZ2, only biotite and muscovite that contain fluorine, whereas in IZ3 fluorine is present in biotite and apatite.

Based on these results, one can surmise that the diversity of fluorine-rich minerals is greater in IZ1 than in the other two zones.

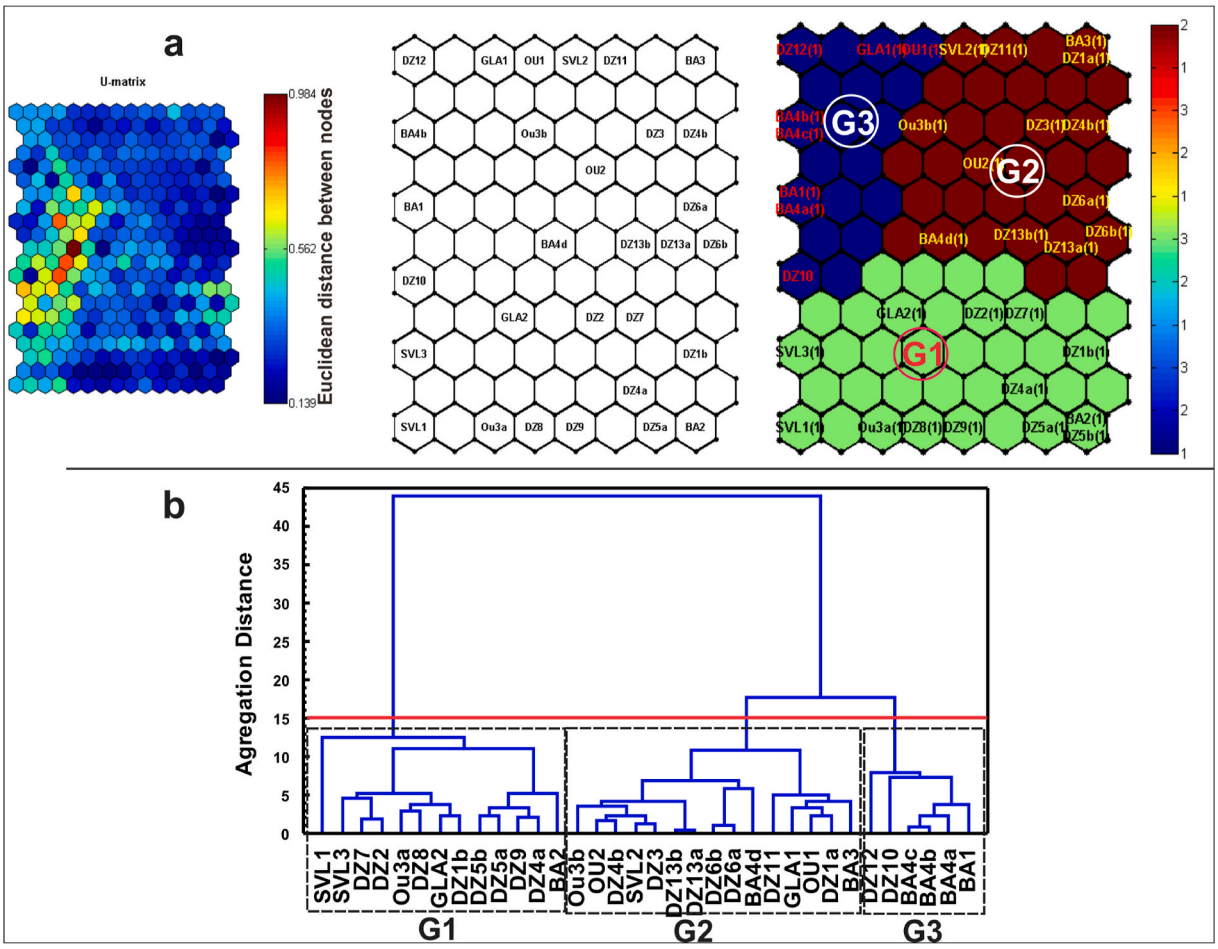


**Fig. 10.** Clustering by (a) U-Matrix through the Self organizing method (SOM) and (b) ascending hierarchical classification (AHC).

fluorine-rich mineral and major elements), it should be noted that for individual samples of G1, fluorine shows a similar pattern with CaO, $Fe_2O_3$, MgO, $P_2O_5$, $TiO_2$ and biotite. These similarities reflect the mineralogical composition of the rocks. Indeed, the similarity between F and $TiO_2$ indicates that parts of the whole-rock F is contained in titanite. The strong similarity between CaO, $P_2O_5$ and F indicates that apatite minerals also contribute to the whole-rock F. Similarly, the similarity between F and CaO patterns reflects the contribution of fluorine ($CaF_2$). Further, similarities between F, $Fe_2O_3$, and MgO confirm the role of biotite, allanite and also other mafic minerals such as amphiboles, although they are scarce in the rock. For samples of G1, it can be concluded that there are wide variety of fluorine-rich minerals involved in the mobilization of fluorine in the rocks.

The samples from G3 (with the lowest fluorine contents) show similar relationships as observed in G1 with the exception that for G3, the similarity between F and CaO is lower whereas fluorine and amphibole are better correlated. It is therefore probable that in the rocks of group 3, fluorine may be mainly linked to the presence of amphibole.

The samples of G2 display less apparent similarity between fluorine and other parameters except with amphibole, but very weakly. This indicates that in the presence of fluorine might be related to potassic minerals such as biotite and muscovite or amphibole.

In summary, the multivariate analysis indicates that high concentrations of fluorine in the rocks (mainly in IZ1) result from the presence of several minerals such as biotite, titanite, apatite, amphibole, muscovite and fluorite. The role of mafic minerals, mainly biotite, are the predominant contributors as shown by the strong similarity between fluorine and biotite and its abundance in this area.

*5.3.2. Quantitative contribution of the various fluorine bearing minerals*

An estimate of the relative quantitative contribution (ppm) of each F-rich mineral to the total fluorine of rock was carried out with a mass balance approach. This approach is based on combining the proportions of each mineral in the rock (in wt. %) with its fluorine concentrations (in wt. %) (Hallett et al., 2015). The F contribution of each mineral is given by the following equation:

$$\mathbf{C_m(ppm) = A_m \times F_m \times 100} \quad \text{Eq. 1}$$

where $\mathbf{C_m}$ is the amount of F (in ppm) contributed by a given mineral to the rock, $\mathbf{A_m}$ represents its abundance/proportion in the rock (in wt. %) and $\mathbf{F_m}$ is the fluorine concentration of this mineral (in wt. %).

The mineral proportions that were used are those obtained by XRD except for fluorite, apatite and muscovite for which the proportions obtained by point counting were used. The results of the estimates are summarized in Table 6 and Fig. 12 presents the relative contribution (in %) of each fluorine-bearing minerals.

Data shown in Table 6 indicate that, in terms of the absolute quantitative contribution at the mineral scale, fluorite provides the highest contribution (max. 2766 ppm), followed by biotite (max. 1776 ppm). The contributions of the other minerals are relatively modest, compared to fluorite and biotite. However, in terms of the relative contribution (in %), when considering the rock scale, the contribution of biotite is clearly dominant (average 70%) (Fig. 12) while the fluorite average contribution is about 47%. Titanite, followed by amphibole, comes after these two minerals. Apatite probably contributes the least (about 4% only) to the bulk fluorine of the whole rock. It is also observed that fluorite, even when present in very low concentration (less than 1%), can contribute

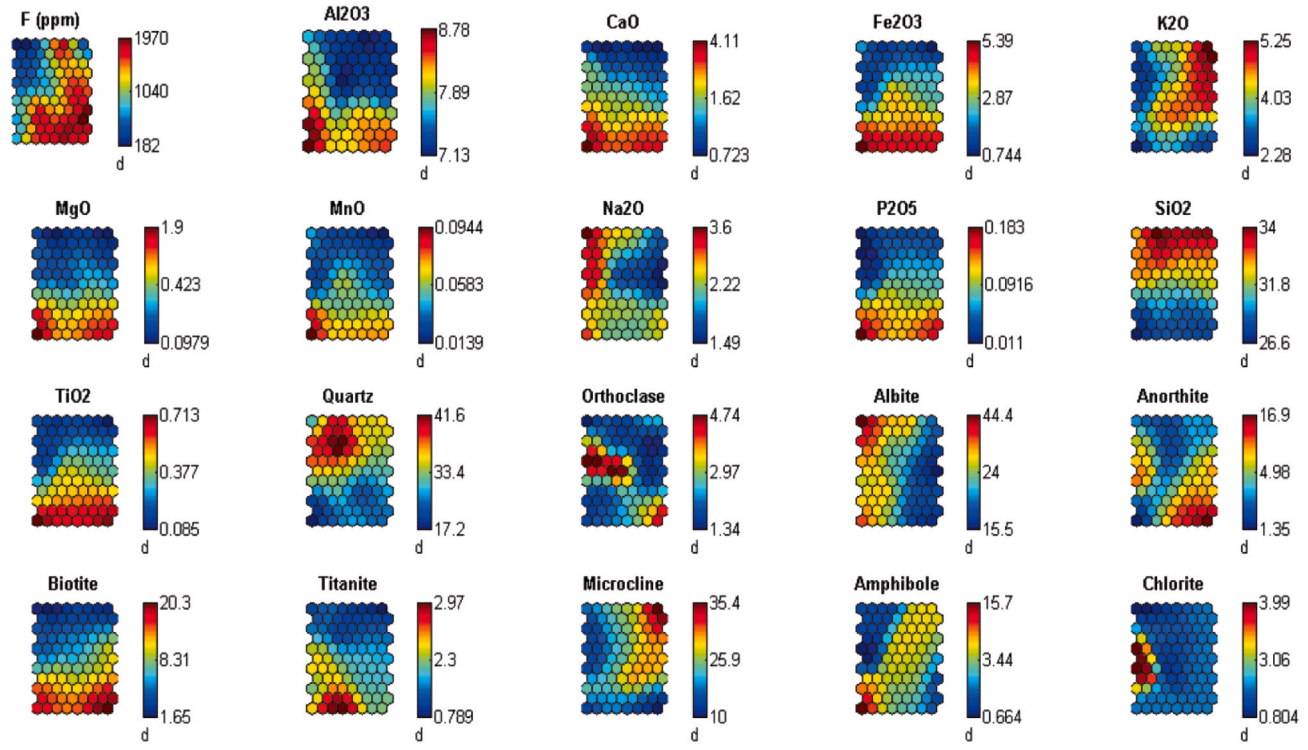


**Fig. 11.** Components matrix after the Self Organizing Map (SOM) indicating the relationship between the fluorine, the various minerals and the major elements. Numbers of the legend of each elements indicate the range of concentration values (wt. % for minerals and major elements; ppm for F).

**Table 6**
Quantification by the mass balance method: statistics summary on fluorine concentration (ppm) of major fluorine rich-minerals.

| | Absolute quantitative contribution (in ppm) of each mineral to total fluorine of the rock ($C_m = A_m \times F_m \times 100$) | | | | | | | Equivalent (in %) of the contribution of each mineral to the total fluorine of the rock | | | | | | |
|---|---|---|---|---|---|---|---|---|---|---|---|---|---|---|
| | Biotite | Muscovite | Amphibole | Sphene. | Fluorite | Apatite | Total | Biotite | Muscovite | Amphibole | Sphene | Fluorite | Apatite | Total |
| **BA2** | 728.00 | 25.28 | 22.50 | - | - | - | **775.78** | 93.84 | 3.26 | 2.90 | - | - | - | **100** |
| **DZ11** | 148.00 | 4.00 | - | - | 2766.07 | - | **2918.07** | 5.07 | 0.14 | - | - | 94.79 | - | **100** |
| **DZ14** | - | - | 708.00 | - | - | 39.12 | **752.72** | - | - | 94.06 | - | - | 5.20 | **99.26** |
| **DZ1b** | 1776.25 | - | 1.50 | 317.00 | 1038.36 | - | **3133.11** | 56.69 | - | 0.05 | 10.12 | 33.14 | - | **100** |
| **DZ2** | 626.40 | - | 119.00 | 176.80 | - | 36.04 | **958.24** | 65.37 | - | 12.42 | 18.45 | - | 3.76 | **100** |
| **DZ5a** | 1510.85 | - | - | 150.80 | - | - | **1661.65** | 90.92 | - | - | 9.08 | - | - | **100** |
| **GLA1** | 14.80 | - | - | - | - | - | **14.80** | - | - | - | - | - | - | |
| **GLA2** | 815.85 | 19.20 | - | 363.25 | - | 20.14 | **1218.44** | 66.96 | 1.58 | - | 29.81 | - | 1.65 | **100** |
| **OU1** | 96.50 | 18.58 | - | - | - | - | **115.08** | 83.86 | 16.14 | - | - | - | - | **100** |
| **SVL1** | 1326.00 | - | 72.15 | - | - | - | **1398.15** | 94.84 | - | 5.16 | - | - | - | **100** |
| **SVL2** | 795.00 | - | - | - | 157.30 | 156.49 | **1108.79** | 71.70 | - | - | - | 14.19 | 14.11 | **100** |

**NB:** The dash indicates cells where the parameters don't exist (could not be measured).

substantially to the total fluorine of the rock. Thus, even as a trace, it may be a potential source of water enrichment in fluoride, especially because of its very high solubility.

When considering the spatial distribution of the various F-rich minerals, biotite may be predominant source as it is much more widespread and abundant than all other fluorine bearing minerals. Thus, biotite is present in all facies and has very appreciable proportion while fluorite, as well as apatite appears localized only in certain parts of IZ1. Therefore, biotite, because of its ubiquitous character and its qualitative and quantitative contribution to fluorine of the whole rock, should be the most important mineral in the fluoride mobilization in the water in the area.

## 6. Conclusions and perspectives

Results of this study have highlighted the significant control of the bedrock mineralogy and texture on the F concentrations of groundwaters in the Department of "Collines" in central Benin. Biotite is the most contributing mineral to elevated fluoride concentrations in groundwater, mainly in the granitic formations. Other fluorinated minerals such as fluorite, fluorapatite, amphiboles, etc. exist and can contribute much smaller proportion of fluoride than biotite.

Previous results have indicated already that the mineralization and fluoride concentrations of groundwater mainly depends upon the basement characteristics (physical and chemical). Results obtained here confirm this initial observation, but they also allow to go one step further in the understanding of the origin of fluoride through the detailed petrological, mineralogical and geochemical characterization of the hosting rock formations. In particular, the spatial differentiation that was observed in groundwater mineralization and fluoride concentrations between the different investigated areas is also evidenced here with differences in the rock compositions and weathering capacity. These observations already allow to improve our capacity to select, based on the local geology, places for drilling new pumping wells in

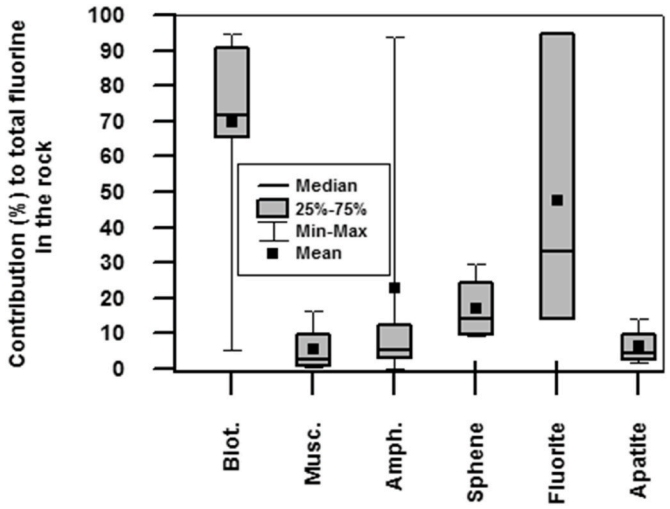


**Fig. 12.** Contribution (%) of each fluorine-rich mineral to the total fluorine in the rock. Biot. = Biotite; Musc. = Muscovite; Amph. = Amphibole; Min-Max = Minimum-Maximum; 25%–75% = 25 - 75th percentiles.

areas where concentrations of fluoride in groundwater are lower than drinking standards.

Having in mind however that the analysis remains based on a relatively limited number of rock samples, most of them sampled from outcrops, a future significant extension to this work will consist in increasing the number of rock sampling points, including as much as possible, rock samples collected from the deeper subsurface during drilling operations, together with groundwater samples from the same locations. Doing so, it is expected that the conclusions drawn here could be more quantitative, with the perspective of improving the geostatistical maps that have already been produced to predict the concentrations of fluoride in groundwater.

## Declaration of competing interest

The authors declare that they have no known competing financial interests or personal relationships that could have appeared to influence the work reported in this paper.

## Acknowledgements

We are indebted to Wallonia Brussels International (WBI), who financially supported this research trough the project: *"Renforcement des capacités relatives à l'exploitation des ressources en eau souterraine au Bénin: Diagnostic de leur qualité et impact de leur consommation sur la santé"*. We would also like to greatly thank people who helped with the new data, in the field and in the lab. Many thanks to anonymous reviewers for the important remarks and comments that helped to improve this paper.

## Appendix A. Supplementary data

Supplementary data to this article can be found online at https://doi.org/10.1016/j.jafrearsci.2021.104301.

## References

Abdelgawad, A.M., Watanabe, K., Takeuchi, S., Mizuno, T., 2009. The origin of fluoride-rich groundwater in Mizunami area, Japan — mineralogy and geochemistry implications. Eng. Geol. 108, 76–85. https://doi.org/10.1016/j.enggeo.2009.06.016.

Adissin Glodji, Luc., 2012. La zone de cisaillement de Kandi et le magmatisme associé dans la région de Savalou-Dassa (Bénin) : étude structurale, pétrologique et géochronologique. Sciences de la Terre. Université Jean Monnet - Saint-Etienne; Université d'Abomey-Calavi (Bénin), 2012. Français. ffNNT : 2012STET4001ff. fftel-00951647.

Adissin Glodji, L., Bascou, J., Yessoufou, S., Ménot, R.-P., Villaros, A., et al., 2014. Relationships between deformation and magmatism in the Pan-African Kandi Shear Zone: Microstructural and AMS studies of Ediacaran granitoid intrusions in central Bénin (West Africa). J. Afr. Earth Sci. 97, 143–160. https://doi.org/10.1016/j.jafrearsci.2014.04.012.

Apambire, W.B., Boyle, D.R., Michel, F.A., 1997. Geochemistry, genesis, and health implications of fluoriferous groundwaters in the upper regions of Ghana. Environ. Geol. 33 (1), 13–24.

Barbé (Le), L., Alé, G., Millet, B., Texier, H., Borel, Y., René, G., 1993. Les Ressources en Eaux Superficiels de la République du Bénin. ORSTOM and Directorate of Hydraulic of Benin, p. 543.

Bell, M.E., Largent, E.J., Ludwig, T.G., Muhler, J.C., Stookey, G.K., 1988. L'approvisionnement de l'homme en Fluor, p. 58.

Bigioggero, B., Boriani, A., Cadoppi, P., Sacchi, R., Vedogbeton, N., Yevidé, H., 1988. Données préliminaires sur les granites du Bénin Méridional. Rendiconti della Soc. Ital. Mineral. Petrol. 4 (1), 477–484.

Boukari, M., 1982. Contibution à l'étude hydrogéologique des régions de socle de l'Afrique Intertropicale: l'Hydrogéologie de la région de Dassa-Zoumé (Bénin). PhD thesis in Applied Geology, specializing in Hydrogeology, University of Dakar (Senegal) 173.

Boussari, W.T., 1975. Contribution à l'étude géologique du socle cristallin de la zone mobile Pan-Africaine (Région centrale du Dahomey). PhD thesis Faculty of Science and Technology. *University of Besançon***135p**.

Breda, 1989. Notice explicative de la carte géologique à 1/200000. Feuilles Pira-Savè, Abomey-Zagnanado, Lokossa-Porto-Novo, p. 77p.

Brinis, N., Boudoukha, A., 2011. Classification statistique et hydrochimique des eaux souterraines de la plaine d'El-Outaya. (W) de Biskra-Algérie. COURRIER DU SAVOIR 11, 41–46.

Chery, L., Larpin, O., 2003. Contribution à la caractérisation des états de référence géochimique des eaux souterraines. Application de la méthodologie à la nappe du Rhin. Rapport BRGM/RP-52163-FR 127p.

Dovonon, L.F.C., Soclo, H.H., Gbaguidi, M.A.N., Youssao, A., 2011. Utilisation des os calcinés dans la défluoruration des eaux contaminées : Détermination expérimentale de la température de calcination et de la granulométrie optimales des os. Int. J. Biol. Chem. Sci. 5 (4), 1712–1726.

Dubroeucq, D., 1977. Notice explicative n°66(5) de la carte pédologique de reconnaissance de la République Populaire du Bénin au 1/200000 - feuille de Parakou. Office de la Recherche Scientifique et Technique Outre-Mer, p. 45.

Dutreuil, J.-P., 1979. Séquence d'altérabilité croissante des granodiorites aux leucogranites orientés dans les arènes des granitoides de l'Ouest de Limousin (Massif Central Français). Norois.n°102 *1979*, 35–246. https://doi.org/10.3406/noroi.1979.3773.

Edmunds, W.M., Smedley, P., 2005. Fluoride in natural waters. In: Selinus, O., Alloway, B., Centeno, J.A., Finkelman, R.B., Fuge, R., Lindh, U., Smedley, P.L. (Eds.), Essentials of Medical Geology : Impacts of the Natural Environment on Public Health. Elsevier, Amsterdam; London, UK, ISBN 0126363412, pp. 301–329.

Faure, P., Volkoff, B., 1996. Différenciation régionale des couvertures pédologiques et litho-géomorphologie sur socle granito-gneissique du Bénin (Afrique Occidentale). Géosciences de surface 322 (IIa), 393–400.

Fawell, J., Bailey, K., Chilton, E., Dahi, E., Fewtrell, L., Magara, Y., 2006. Fluoride in Drinking-Water. World Health Organization-WHO), IWA Publishing, London, UK, 1900222965.

Ge, Zhu, Xiong, Wu, Jianping, Ge, Fei, Liu, Weiguang, Zhao, Chu, Wu, Weiguang, Zharo, Chu, Wu, et al., 2020. Influence of mining activities on groundwater hydrochemistry and heavy metal migration using a self-organizing map (SOM). J. Clean. Prod. 257 (2020) https://doi.org/10.1016/j.jclepro.2020.120664.

Giraudel, J.L., Lek, S., 2001. A comparison of self-organizing map algorithm and some conventional statistical methods for ecological community ordination. Ecol. Model. 146 (1), 329–339. https://doi.org/10.1016/S0304-3800(01)00324-6.

Goldich, S., 1938. A study in rock weathering. J. Geol. 46 (1), 17–58. https://doi.org/10.1086/624619.

Guihéneuf, N., Boisson, A., Bour, O., Dewandel, B., Perrin, J., Dausse, A., Viossanges, M., Chandra, S., Ahmed, S., Maréchal, J.C., 2014. Groundwater flows in weathered crystalline rocks: impact of piezometric variations and depth-dependent fracture connectivity. J. Hydrol. 511, 320–334. https://doi.org/10.1016/j.jhydrol.2014.01.061.

Gunnar, J., Prosun, B., Vikas, C., Singh, K.P., 2005. Controls on the genesis of some high-fluoride groundwaters in India. Appl. Geochem. 20, 221–228. https://doi.org/10.1016/j.apgeochem.2004.07.002.

Hallett, B.M., Dharmagunawardhane, H.A., Atal, S., Valsami-Jones, E., Ahmed, S., Burgess, W.G., et al., 2015. Mineralogical sources of groundwater fluoride in Archaen bedrock/regolith aquifers: Mass balances from southern India and north-central Sri Lanka. J. Hydrol.: Region. Stud. 4, 111–130. https://doi.org/10.1016/j.ejrh.2014.10.003.

Handa, B.K., 1975. Geochemistry and genesis of fluoride-containing groundwater in India. Groundwater 13 (3), 275–281. https://doi.org/10.1111/j.1745-6584.1975.tb03086.x.

Hayes, T.S., Miller, M.M., Orris, G.J., Piatak, N.M., II, 2017. Fluorine. In: Schulz, K.J., DeYoung Jr., J.H., Seal, R.R. (Eds.). In: Bradley, D.C. (Ed.), Critical Mineral Resources of the United States - Economic and Environmental Geology and Prospects for Future Supply. Chapter G. *U.S. Geological Survey, Professional Paper 1802*, pp. G1–G80. https://doi.org/10.3133/pp1802G.

Hem, J.D., 1985. Study and interpretation of the chemical of natural water. U.S Geological Survey Water-Supply 2254, 255.

Hoareau, J.-L., Nicolini, E., Fritz, B., Delcher, E., 2005. Signatures géochimiques des eaux souterraines en milieu basaltique tropical (île de la Réunion). Approche expérimentale. Bull. Soc. géol. France 176 (3), 257–267. https://doi.org/10.2113/176.3.257.

Igue, A.M., Weller, U., 2001. Géologie et géomorphologie du Sud Bénin. 9p. https://projekte.uni-hohenheim.de/atlas308/c_benin/projects/c2_1_1/html/french/btext_fr_c2_1_1.htm.

INSAE, 2013. Résultats provisoires du 4ème Recensement Général de la Population et de l'l'Habitat (RGPH4). *Ministère du Développement, de l'Analyse Economique et de la Prospective(République du Bénin)*, p. 8.

Josephus Thomas, J., Glass, H.D., White, W.A., Trandel, R.M., 1977. Fluoride content of clay minerals and argillaceous earth materials. Clay Clay Miner. 25, 278–284. https://doi.org/10.1346/CCMN.1977.0250405.

Kalteh, A.M., Hjorth, P., Berndtsson, R., 2007. Review of the self-organizing map (SOM) approach in water resources: analysis, modelling and application. Environ. Model. Software 23 (7), 835–845. https://doi.org/10.1016/j.envsoft.2007.10.001.

Kamagaté, B., Mariko, A., Seguis, L., Dao, A., Bokar, H., Gone, D.L., 2010. Différenciation hydrogéochimique entre les nappes superficielles des altérites et profondes du socle fissuré dans le bassin versant de Kolondièba (sud du Mali) : approche statistique par la méthode SOM des réseaux de neurones. In: Servat Eric, Demuth S, Dezetter Alain, Daniell, T. (Eds.), Ferrari E. (collab.), Ijjaali M. (collab.), Jabrane R. (collab.), Van Lanen H. (collab.), Huang Y. (collab.). Global Change : Facing Risks and Threats to Water Resources. Proceedings of the Sixth World FRIEND Conference. Wallingford : AISH, 365-373. (AISH Publication ; 340). World FRIEND Conference : Global Change : Facing Risks and Threats to Water Resources, vol. 6, 978-1-907-161-13-1, ISSN 0144-7815Fez (MAR), 2010/10/25-29.

Karro, E., Uppin, M., 2013a. Lithological influences on occurrence of elevated boron and fluoride levels in groundwater. In: Oral Presentation at the 8th IAHS International Groundwater Quality Conference, Gainesville, Florida USA, 13 Slides.

Karro, E., Uppin, M., 2013b. The occurrence and hydrochemistry of fluoride and boron in carbonate aquifer system, central and western Estonia. Environ. Monit. Assess. 185, 3755. https://doi.org/10.1007/s10661-012-2824-5, 3748.

Kim, K.-H., Yun, S.-T., Yu, S., Choi, B.-Y., Kim, M.-J., Lee, K.-J., 2020. Geochemical pattern recognitions of deep thermal groundwater in South Korea using self-organizing map: identified pathways of geochemical reaction and mixing. J. Hydrol. 589, 125202. https://doi.org/10.1016/j.jhydrol.2020.125202.

Kohonen, T., 1982. Self-organized formation of topologically correct feature maps. Biol. Cybern. 43, 59–69.

Kohonen, T., 1998. The self-organizing map. Neurocomputing 21 (1998), 1–6. https://doi.org/10.1016/S0925-2312(98)00030-7.

Kyung-Jin, L., Seong-Taek, Y., Soonyoung, Y., Kyoung-Ho, K., Ju-Hee, L., Seung-Hak, L., 2020. The combined use of self-organizing map technique and fuzzy c-means clustering to evaluate urban groundwater quality in Seoul metropolitan city, South Korea. J. Hydrol. 569 (11), 685–697. https://doi.org/10.1016/j.jhydrol.2020.125655.

Ladouche, B., Chery, L., Petelet-Giraud, E., 2004. Contribution à la caractérisation des états de référence géochimique des eaux souterraines. Application de la méthodologie en milieu de socle fracturé (Naizin, Morbihan), p. 67. Report - BRGM/RP-53025-FR.

Lahermo, P., Backman, B., 2000. The occurrence and geochemistry of fluorides with special reference to natural waters in Finland. Geological Survey of Finland, Report of Inverstigation 149 (2000), 40. **ISBN951-690-757-1**.

María, G.G., Laura, B., 2015. Chapter 1: fluoride in the context of the environment. In: Fluorine: Chemistry, Analysis, Function and Effects, ISBN 978-1-78262-850-7, pp. 3–21. https://doi.org/10.1039/9781782628507-00003.

Missi, C., Atekwana, E.A., 2020. Physical, chemical and isotopic characteristics of groundwater and surface water in the Lake Chilwa Basin, Malawi. J. Afr. Earth Sci. 162, 103737. https://doi.org/10.1016/j.jafrearsci.2019.103737.

Oloukoi, J., Mama, V.J., Agbo, F.B., 2006. Modélisation de la dynamique de l'occupation des terres dans le département des Collines au Bénin. Teledetection 6 (4), 305–323.

Peeters, L., Bacao, R., Lobo, V., Dassargues, A., 2007. Exploratory data analysis and clustering of multivariate spatial hydrogeological data by means of GEO3DSOM, a variant of Kohonen's Self-Organizing Map. Hydrol. Earth Syst. Sci. 11 (4), 1309–1321. https://doi.org/10.5194/hess-11-1309-2007, 2007.

Rondeau, A., 1960. Altération comparée des granites et des gneiss dans le Morvan. Annales de Géographie.t.69, n°376 **617**–618. https://doi.org/10.3406/geo.1960.14777.

Susheela, A.K., Keast, G., 1999. Fluoride in water: an overview. Water Front 199 (13), 11–13.

Tossou, Y.Y.J., 2016. Caractérisation des anomalies fluorées eaux souterraines du socle cristallin Précambrien du Bénin central (Afrique de l'Ouest). Apport des outils hydrogéochimiques, petrographiques et minéralogiques. PhD thesis in Engineering Sciences, University of Liege 181.

Tossou, Y.Y.J., Orban, P., Gésels, J., Yessoufou, S., Boukari, M., Brouyère, S., 2017. Hydrogeochemical mechanisms governing the mineralization and elevated fluoride ($F^-$) contents in Precambrian crystalline aquifer groundwater in central Benin, Western Africa. Environmental Earth Sciences 76, 691. https://doi.org/10.1007/s12665-017-7000-3.

Tossou, Y.Y.J., Hermans, T., Dovonon, L.F., Orban, P., Boukari, M., Brouyère, S., 2019. Proposal of a decision support for accessing to improved groundwater quality in a context of fluoride geogenic contamination in Bénin, Western Africa. Geo-Eco-Trop 43 (3), 365–373, 2019.

Ultsch, A., Siemon, H.P., 1989. Exploratory Data Analysis: Using Kohonen Networks on Transputers. Research Report N° 329. University of Dortmund.

Ultsh, A., Herrmann, L., 2005. *The Architecture of Emergent Self-Organizing Maps to Reduce Projection Errors. ESSANN2005 13th European Symposium On Artificial Neural Networks*. Bruges, Belgium, pp. 1–6.

WHO, 2017. Guidelines for Drinking-Water Quality: Fourth Edition Incorporating the First Addendum. World Health Organization, Geneva, p. 631, 2017. Licence: CC BY-NC-SA 3.0 IGO.

WHO, 2018. Developing Drinking-Water Quality Regulations and Standards: General Guidance with a Special Focus on Countries with Limited Resources. World Health Organization, Geneva, p. 68, 2018. Licence: CC BY-NC-SA 3.0 IGO.